NON-LINEAR ANALYSIS OF STEEL FIBER REINFORCED CONCRETE HOLLOW COLUMNS UNDER UNIAXIAL BENDING

by

MOHAMMED HUZAIFA GHORI

Presented to the Faculty of the Graduate School of

The University of Texas at Arlington in Partial Fulfilment

of the Requirements

for the Degree of

MASTER OF SCIENCE IN CIVIL ENGINEERING

THE UNIVERSITY OF TEXAS AT ARLINGTON

December 2017

Acknowledgement

I would like to offer my sincere appreciation to Dr. Raad Azzawi for his guidance and support throughout my graduate academic career. He has been a wonderful mentor to me, providing invaluable technical and academic guidance over the course of this research. His knowledge and advice has always provided me with great inspiration and motivation in dealing with academic and personal challenges. I would also like to thank Ghassan who provided me with invaluable support and assistance throughout the course of this project. Appreciations are also extended to Dr. Shahandashti and Dr. Ham for their valuable advice and guidance.

I would like to thank my parents, who have always provided great encouragement and support helping me overcome some of the greatest challenges.

December 22, 2017

Abstract

NON-LINEAR ANALYSIS OF STEEL FIBER REINFORCED CONCRETE HOLLOW COLUMNS UNDER UNIAXIAL BENDING

Mohamed Ghori, MS

The University of Texas at Arlington, 2017

Supervising Professor: Raad Azzawi

This study investigates the performance of Steel Fiber Reinforced concrete hollow columns under axial compressive load and uniaxial bending with varying amounts of steel fiber using Finite Element Method of Analysis. The columns are of two groups, one with a 10% void and the other group has 20% void at the center. Each group's specimens' fiber content is varied in 0.5% increments from 0 to 1.5%.

Also, the collapse load of the columns was obtained. Numerical results were compared with the available experiments. Two parametric studies were conducted by varying the amount of void percentages and steel fiber contents. In the first study, a 30% hollow section was analyzed by varying steel fiber content in 0.5% increments from 0.5% to 2.5%. Secondly, the hollow opening for 10%, 20% and 30% was compared with a constant steel fiber of 1.5% by volume.

It was observed that introduction of a hollow opening reduces the capacity of the section and the loss in strength is proportionate to the opening size. Adding steel fibers provide ductility to the section by increasing the first-cracking load and also increasing the collapse load of the specimen. For openings within 10%, adding 0.5% steel fibers by volume yields strength results similar to a solid section without any steel fibers, and for openings within 20%, adding 1.5% steel fibers by volume yields strength results similar to a solid section without any steel fibers. Similar results were observed in the parametric study.

Table of Contents

List of Figures

List of Tables

Chapter 1

Introduction

Reinforced Concrete is one of the most popular material used for constructing a wide range of bridges, buildings and other structures due to it's advantages such as durability, high strength, easy to cast in unique shapes and economy. An increase in the demand of constructing high rise concrete structures led people to use high strength concrete instead of normal strength concrete, to get stronger concrete structures and to minimize the size and weight of concrete members in the structure.

Increased ductility in concrete structures will allow the structure to display failure signs and warn populists that the structure could fail in turn to save lives. In order to increase the strength and ductility of concrete and to maximize structural efficiency in terms of strength to mass and stiffness to mass ratios, and to reduce contribution of the columns to seismic response and high carrying demand on foundation it is desirable to use advanced concrete strength, structural longevity, and to reduce the weight of concrete members (Azzawi 2017).

By applying steel fibers in concrete members, no significant increase in weight of structure will occur, however, it significantly enhances the concrete structure's performance especially in terms of strength and ductility. In location where high seismic activity and natural boundaries require high-elevation infrastructures, hollow columns can be the solution to reduce the mass contribution of column to the seismic response. Holes are often provided in reinforced concrete columns to allow access for services of plumbing and electric wiring. Also in some industrial buildings these pipes may carry liquids or gases which are very harmful to the safety of the buildings in case of fire. The provision of such openings in reinforced concrete columns may cause a loss of strength and stiffness and hence, significant structural damage may be sustained, if the provision of the openings is not checked carefully during the design or construction stages (Azzawi 2017).

However, current standards of practice have not answered specific problems regarding new designs of hollow section columns, while hollow columns have already been used in many existing buildings and bridge piers.

1.1 Objectives

Reinforced Concrete is the backbone of this era's infrastructure. With the changing technologies, a lot of study is being done on improving and enhancing the performance of our structures. The use of hollow columns is still scarce. Hollow columns provide facility of embedding pipes and ducts. They may be used to maximize structural efficiency in terms of stiffness to mass ratio. They may also be used where the weight of concrete members is to be kept to a minimum, where the cost of concrete is relatively high.

The ACI-318 Building Code provides design aids for Rectangular and Circular cross-sectioned RCC Columns. However, there is no mention of either shape including a hollow opening.
This paper develops fundamental knowledge of using steel fibers in hollow columns with different sizes of holes and steel fiber content under eccentric loading, so that the different behavior can be identified. This study has gone as far up to 30% void. Meaning reducing the amount of concrete in column cross-section by 30%. This results in huge saving in concrete costs and ease on-site in creating forms and pouring concrete.

1.2 Research Contribution

Concrete, inherently is a composite material that is strong in compression and weak in tension. Although the recent advancements in concrete technology has increased the compressive strengths of concrete significantly, it still fails to overcome the brittle nature of concrete. Fiber-reinforced concrete (FRC) has attracted a considerable amount of research in the past few decades and has demonstrated promising potential in being a major element for refining future structural design methods and practices. To foster the compressive strength without sacrificing

the ductility, a strategy is to add discrete steel fibers. These fibers provide the tensile strength that the concrete member lacks.

As the steel fiber-reinforced concrete hardens, shrinks, or bears service loads to develop cracks and to propagate them, the fibers evenly distributed throughout the composite intersect, block, and even arrest the propagating cracks This way, the addition of fibers contributes strength to the concrete. The fibers used in the experiment are a low carbon drawn wire. Steel fiber dosages ranged from 0% to 1.5% by volume. In the numerical model, the fiber dosage was increased up to 2.5%.

Numerical analyses were conducted and the results were compared with the available lab experiments. In future, researchers may modify the parameters of the specimen and conduct parametric studies. This in turn saves the time and cost of conducting repetitive lab experiments.

1.3 Outline for Thesis

This thesis is presented in five chapters. A brief description of each Chapter is provided below;

Chapter 1 — Introduction

This chapter presents the introduction to the thesis, important facts are mentioned here that led to pursue research in the specified area.

Chapter 2 — Literature Review

In this chapter, the present knowledge background is studied which is used as a base upon which the thesis is done.

Chapter 3 — Finite Element Method of Analysis

This chapter discusses background of FEM Modelling and the steps taken in order to develop the specimen models.

Chapter 4 — Numerical Analysis

This chapter presents the results and load versus lateral mid-height deflection curves for each specimen of every group.

Chapter 5 — Summary and Conclusions

This chapter summarizes the work done with conclusions and recommendations for future study.

Chapter 2

Literature Review

2.1 Hollow Columns and Steel Fibers

Azzawi and Abolmaali (2017) investigated experimentally the behavior of Steel Fiber Reinforced Concrete Columns with openings under eccentric loading. The experimental results of testing of nine hollow concrete columns with square cross sections was presented. It was found that adding steel fibers increases first cracking load and prevents premature failure of concrete leading to significant improved performance of Reinforced Concrete Hollow Columns.

When using a hollow section instead of a solid section, the hollow core section enables to maintain a good strength strength/mass and stiffness/mass relationship, because it is maintaining a high moment of inertia while reducing its mass, (Qiang et al 2013). The use of less mass is beneficial in seismic design of high-rise concrete structures since the large movements in the lateral direction will cause large second order effects (Model Code 2010).

Hollow sections provide enough axial loading area to resist the low axial loads applied to columns in seismic regions, as well as providing concrete and reinforcing steel where they will be more effectively utilized. These sections are able to greatly reduce the mass of the column, as well as the amount of materials used to construct the column. The reduction in mass can also help improve the seismic response, since the response will have a smaller mass contribution (Ryan Beck 2014).

Reinforcement detailing in hollow sections are more complicated than solid sections, correct spacing and constructability of these sections need to be properly and crucial to ensure a ductile behavior of the structure if extreme loads are applied such as strong earthquakes, (Subramanian 2011). Another important aspect is the arrangement of the reinforcement within the plastic hinge region where transverse reinforcement should be designed to avoid shear

failure, splitting failure in anchorage zones, prevent buckling of longitudinal bars and to effectively confine the concrete in order to ensure a ductile behavior when failing. (Paultre & Legeron 2008).

Wilson and Abolmaali (2013) compared the test results for material behavior for zero slump dry cast steel and synthetic fiber reinforced concrete beam. Their study investigated the material properties comprising; compressive strength, peak load, modulus of rupture and specimen toughness. Load-deformation plots were obtained and it was observed that low dosages of fiber displayed significant drop in load after the first-crack. Higher dosages showed strain hardening after a slight drop in load due to the first-crack.

Shende and Pande (2011) investigated the effects of steel reinforced concrete beams for flexural and deflection comparisons. Three steel fibers used had aspect ratios of 50, 60 and 67. The concrete mixture was constant except for the change in fiber dosages of 0%, 1%, 2%, and 3% by volume. It was determined that the addition of steel fibers increased the flexural strength compared to the plain concrete by 8.80-10.40 MPa, 8.40-10.00 MPa, and 8.27-9.73 MPa for 1%, 2%, and 3% by volume of steel fibers, respectively. The variations in the flexural strength are due to the change in aspect ratio and increase as the ratio increases. Deflection curves followed similar patterns for all fiber types and fiber dosages with a noticeable reduction for 3% of steel by volume.

Bodin et al.(2002), proposed a non-linear finite element (FE) analysis in order to complete the experimental analysis of the flexural behavior of the beams. Elasto-plastic behavior was assumed for reinforced concrete and interface elements were used to model the steel concrete bond and the adhesive. A numerical analysis also included simulations on pre-cracked beams.

Nagarnaik and Pande (2011) conducted a series of compression tests on various specimens using a modified test that gave the complete compressive strength, static, dynamic modulus of elasticity and stress-strain behavior using silica fume with and without steel fiber of volume

fractions 0, 0.5, 1.0, and 1.5% of 0.5mm diameter of aspect ratio 60 on Portland Pozzolona cement concrete. As a result, the incorporation of steel fibers, silica fume and cement produced a strong composite with superior crack resistance, improved ductility and strength behavior prior to failure. Addition of fibers provided better performance for the cement-based composites.

Y. K. Yeh et al (2002) performed experimental results for two prototypes and four scaled model hollow bridge columns. Primary parameters considered for the specimens were axial load, the amount lateral reinforcement, and height-to-depth ratio. In this study, a specially designed test setup was used to subject the hollow bridge columns to a constant axial load, as well as cyclic transverse shear and bending. Analytical model is also presented that is verified by experimental results. A specimen with greater axial force has less ductility. When the columns are satisfied by the ACI Code, their failure mode is flexure due to rupture of longitudinal rebars. When the amount of lateral reinforcement is less than one half of that required by the ACI Code, the failure mode may become flexure-shear or shear. The analytical model satisfactorily predicts the moment-curvature relationship and load-displacement relationship of all specimen with acceptable accuracy.

Dr. Alaa K. Abdal Karim et al (2013) aimed at presenting simplified approach to enable construction of new design charts for hollow section reinforced concrete columns subjected to an axial compressive load and uniaxial bending. These charts can be directly used in design of hollow column sections, to determine required amount of steel in addition to column dimensions and estimation of column load capacity.

Abhay (2014) performed the study of structural behavior of Hollow (Box-type) and Solid Reinforced concrete members in the RCC framed building under seismic load using ETABS Software. He concluded that maximum node displacement of hollow members given by ETABS is less as compared to solid members. 20% to 27% reduction in the story overturning moment due to hollow members in RCC framed building was observed. Story shear for RCC framed building having hollow members is decreased by 27% as compared to solid members. 74.16

ton of M30 concrete is saved by using hollow (Box-type) members in RCC framed building so it leads to economical design without the failure of the structure against seismic loads.

Jun-ichi Hoshikuma and M.J.N. Priestley (2000) presented the study of flexural ductility capacity of the hollow circular columns with one layer of longitudinal and transverse reinforcement placed near the outside face of the section. The behavior of two-flexure dominant circular hollow reinforced concrete columns, with different longitudinal reinforcement ratios, under cyclic loading was investigated through a discussion of experimental studies. They concluded that the inside face concrete compression strain is one of the most important parameters to control the ductility capacity of the hollow columns. Test results inside face concrete was crushed when the compression strain reached nearly 0.005 even though a sufficient amount of steel was placed near outside face.

Ho-Young Kim et al (2015) conducted study on different specimens for hollow reinforced concrete bridge piers. They concluded that failure behavior of circular hollow RC Bridge pier was referable to the location of the neutral axis at failure. When the neutral axis was located inside the wall section, i.e. between the inside face and outside face of the wall, the inside face of the wall did not show any damages and the columns showed very ductile behavior. The section with this type of failure mode may be called “flexure-controlled section”. However, if the neutral axis was located inside the hollow, i.e. the depth of the neutral axis was greater than the wall thickness, relatively brittle failure was observed due to the concrete crushing and spalling of the inside face of the circular wall. The section with this type of failure mode may be called “compression-controlled section”.

Since the early 1960s there has been an increase in the demand for stronger stiffer and more lightweight materials for use in the aerospace, transportation and construction industries. High performance demands on engineering materials have led to the extensive research and development of new and improved materials, such as composites. Composite materials used for structural purposes often have low densities, resulting in high stiffness to weight and high

strength to weight ratios when compared to traditional engineering materials. In addition to the high fatigue strength to weight ratio and fatigue damage tolerance of many composites also makes them an attractive option.

2.2 Effect of Fibers in Concrete

Fibers are usually used in concrete to control cracking due to plastic shrinkage and to drying shrinkage. They also reduce the permeability of concrete and thus reduce bleeding of water. Some types of fibers produce greater impact, abrasion, and shatter–resistance in concrete. Generally, fiber do not increase the flexural strength of concrete, and so cannot replace moment–resisting or structural steel reinforcement. Indeed, some fibers actually reduce the strength of concrete.

In general, it is difficult to prevent concrete from cracking because it is a non-ductile and brittle material. The formation of cracks, even micro cracks, from loading and environmental effects, has been shown to lead to deterioration and in some cases failure. Micro cracks usually form at the interface of coarse aggregates due to thermal and moisture activity in the cement paste even before loading occurs. Upon loading, these micro cracks propagate and group to form cracks. Short fibers evenly dispersed throughout the concrete increase the durability of concrete by preventing the micro cracks from widening and spreading into larger cracks.

The amount of fibers added to a concrete mix is expressed as a percentage of the total volume of the composite (concrete and fiber), termed "volume fraction" (Vf). Vf typically ranges from 0.1 to 3%. The aspect ratio (l/d) is calculated by dividing fiber length (l) by its diameter (d). Fiber with a non-circular cross section use an equivalent diameter for the calculation of aspect ratio. If the fibers modulus of elasticity is higher than the matrix (concrete or mortar binder), they help to carry the load by increasing the tensile strength of the material. Increasing the aspect ratio of the fiber usually segments the flexural strength and toughness of the matrix. However, fibers that are too long tend to "ball" in the mix and create workability problems.

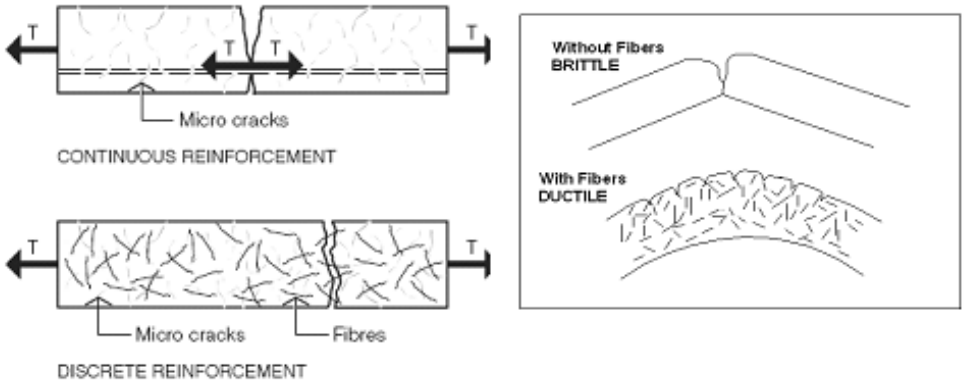

Figure 2.1 Effect of Steel Fibers in Concrete

Figure 2.1 shows the effect of steel fibers in the concrete mix. The steel fibers act as barriers and arrest the growth of tensile cracks. The effect of fibers in the analysis is included by varying the tensile and compressive properties of concrete. These values are obtained from the lab experiments.

2.3 Advantages of Fiber Reinforced Concrete

Fiber reinforced concrete (FRC) has started finding its place in many areas of civil infrastructure applications especially where the need for repairing, increased durability arises. FRC is used in civil structures where corrosion is to be avoided at the maximum. Fiber reinforced concrete is better suited to minimize capitation/erosion damage in structures such as sluice ways, navigational locks and bridge piers where high velocity flows are encountered. A substantial weight saving can be realized using relatively thin FRC sections having the equivalent strength of thicker plain concrete sections. When used in bridges it helps to avoid catastrophic failures. In the quake prone areas, the use of fiber reinforced concrete would certainly minimize the human casualties. Fibers reduce internal forces by blocking microscopic cracks from forming within the concrete (Syed Faiz 2013).

The presence of fiber has a direct effect on the mechanical properties of concrete including compression, direct tension, shear, and flexural strength. The fiber shares induced stress with the concrete until the concrete cracks. Then, eventually the fiber carries all of the stress. There are many advantages that suggest the reduction or replacement of conventional reinforcing steel with steel fibers, such as the following:

• Enhanced flexural strength, shear strength, ductility and toughness.

• Impact and fracture resistance.

• Internal stresses are more evenly distributed throughout the structure because multi-directional reinforcement is provided.

• Crack widths are minimal, if cracks are found at all, because fibers bridge the cracks.

• Decreased chance of corrosion due to crack control and the fact that fibers do not provide a continuous path for corrosive currents to flow through.

• Savings in labor and time costs of a project because FRC placement is less demanding than conventional rebar placement (Syed Faiz 2013).

Chapter 3

Finite Element Method of Analysis

3.1 Introduction

The finite element method is a numerical method for solving problems of engineering and mathematical physics. Typical problem areas of interest in engineering and mathematical physics that are solvable by use of the finite element method include structural analysis, heat transfer, fluid flow, mass transport, and electromagnetic potential.

The Finite Element Analysis of this thesis was conducted using the computer application, Abaqus.

3.2 Modern Development of FEM

The modern development of the finite element method began in the 1940s in the field of structural engineering with the work of Hrennikoff in 1941 and McHenry in 1943, who used a lattice of one-dimensional elements for the solution of stresses in continuous solids. Courant proposed setting up the solution of stresses in a variational form. Then he introduced piecewise interpolation functions over triangular sub regions making up the whole region as a method to obtain approximate numerical solutions. In 1947, Levy developed the flexibility of force method, and in 1953 his work suggested that the stiffness or displacement method could be a promising alternative for use in analyzing statically redundant aircraft structures. However, his equations were difficult to solve by hand, and this the method became popular only with the arrival of the high-speed digital computer. In 1954, Argyris and Kelsey developed matrix structural analysis methods using energy principles. This development illustrated the vital role that energy principles would play in the finite element method (Daryl L. Logan 2007).

Most of the finite element work up to the early 1960s dealt with small strains and small displacements, elastic behavior and static loadings. However, large deflection and thermal

analysis were considered by Turner et al. in 1960 and material non-linearities by Gallagher et al. in 1962, whereas buckling problems were initially treated by Gallagher and Padlog in 1963. Zienkiewicz et al. extended the method to cisco-elasticity problems in 1968. From the early 1950s to the present, enormous advances have been made in the application of the finite element method to solve complicated engineering problems. The development of the computer resulted in the writing of computational programs. A great number of special-purpose and general-purpose programs have been written to handle various complicated structural and non-structural problems. Programs such as ANSYS, ABAQUS, NISA FEA etc. illustrate the elegance of the finite element method and reinforce understanding of it. In fact, finite element programs now can be solved on a single-processor machines, such as a Laptop computer, PC or on a cluster of computer nodes. The powerful processing and storage capacity of computers and the advances in solver programs have made it possible to solve problems with over a million unknowns (Daryl L. Logan 2007).

To use the Finite element method through computer program, the user inputs information such as position of the element nodal coordinates, the manner in which the elements are connected, material properties, applied loads, boundary conditions and the kind of analysis to be performed. The computer then uses this information to generate and solve the equations necessary to carry out the analysis. The finite element is a numerical method for solving problems of engineering and mathematical physics. Common problem areas of interest in engineering and mathematical physics that are solvable by use of the finite element method include structural analysis, heat transfer, fluid flow, and electromagnetic potential (Daryl L. Logan 2007).

For problems including complex geometries, loadings and material properties, it is generally not possible to obtain analytical mathematical solutions. Analytical solutions are those given by a mathematical expression that yields the values of the desired unknown quantities at any location in a body and are thus valid for an infinite number of locations in the body. The finite element formulation of the problem results in a system of simultaneous algebraic equations for the solution, rather than requiring the solution of differential equations. The solution for

structural problems typically refers to determining the displacements at each node and the stresses within each element making up the structure that is subjected to applied loads. The finite element method involves modelling the structure using small interconnected elements called finite elements. A displacement function is associated with each finite element. Every interconnected element is linked, directly or indirectly, to every other element through common interfaces, including nodes and/or boundary lines and/or surfaces. By using known stress/strain properties for the material making up the structure, one can determine the behavior of a given node in terms of the properties of every other element in the structure (Daryl L. Logan 2007).

3.3 Modelling Steps using Abaqus

3.3.1 Creation of Parts

In this step, each part is geometrically sketched and then extruded in the third-dimension axis. Figure 3.1 shows the longitudinal and cross section of a typical specimen.

Every model used in this study has a total of four parts namely;

- Concrete Column

  The dimensions of the column were 200x200x1600 mm

  There are three types of columns; solid, 10%, 20% and 30% hollow section.

  10% hollow - 20x20mm void at the center of the column.

  20% hollow - 40x40mm void at the center of the column.

  30% hollow - 60x60 mm void at the center of the column.

  The concrete column is modelled as a Three Dimensional Deformable solid. An 8 noded linear hexahedral brick element with reduced integration and hourglass control was used to model the specimen in this study

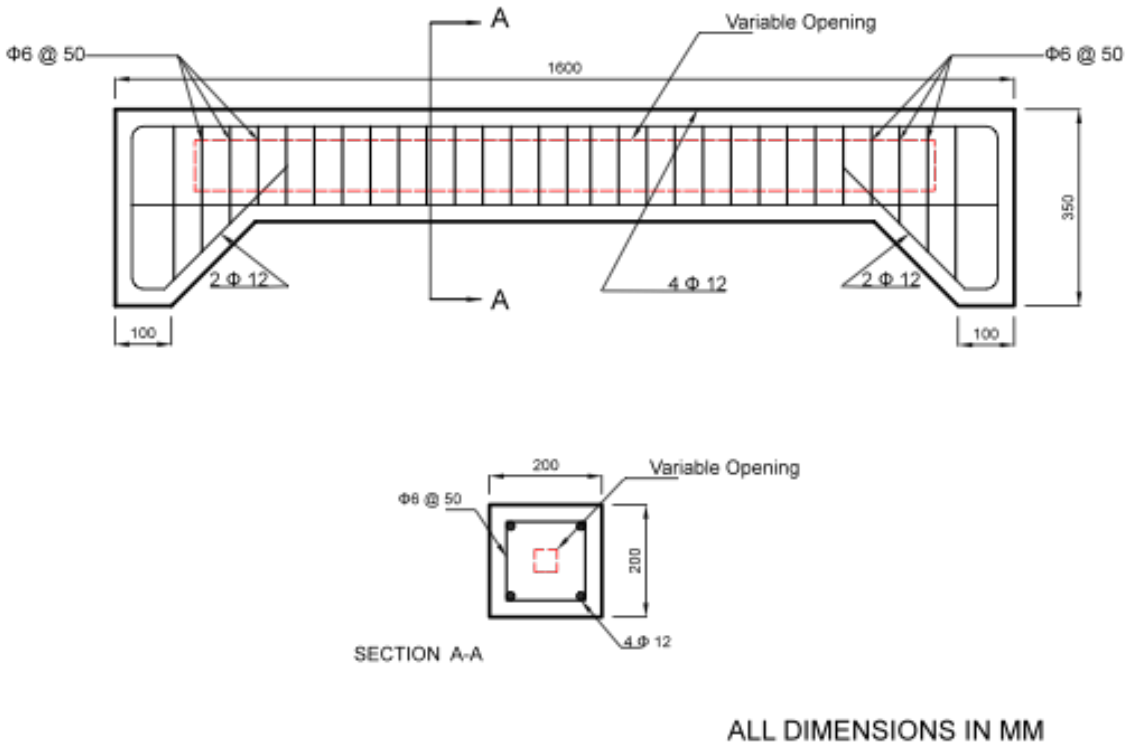

Figure 3.1 Longitudinal and Cross section of a typical specimen

- Longitudinal Reinforcement

  4 Φ12mm bars - Grade 60

- Ties

  Φ6mm @ 50mm spacing - Grade 60

- Pedestal

  In the numerical model, the column specimen rests on a concrete pedestal having dimensions 500x500x250 mm.

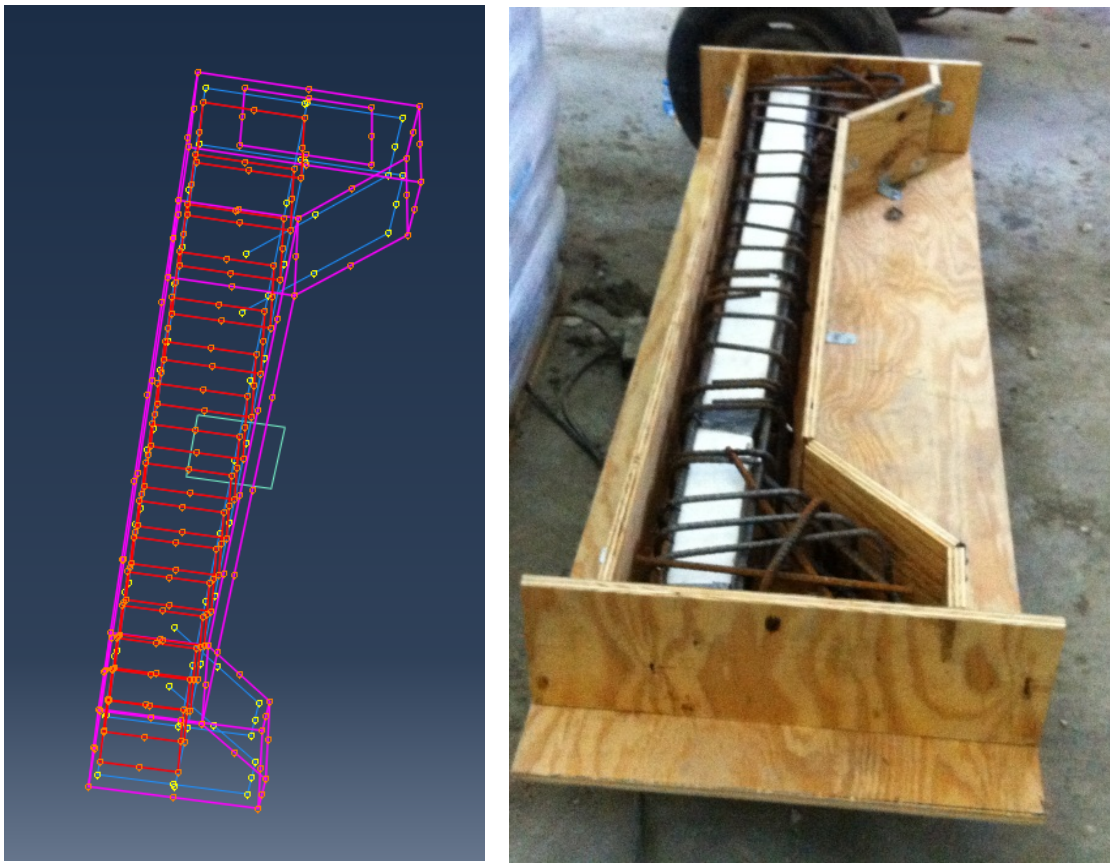

Figure 3.2 Steel Reinforcement Modelled in Abaqus and Experimentally (Azzawi 2017)

The reinforcement is sketched as wire section and it is assigned a cross-sectional area in the section properties. After all the parts are sketched and modelled, the reinforcement is embedded inside the concrete column in the constraint module. The reinforcement is the embedded region while the concrete column is the host region.

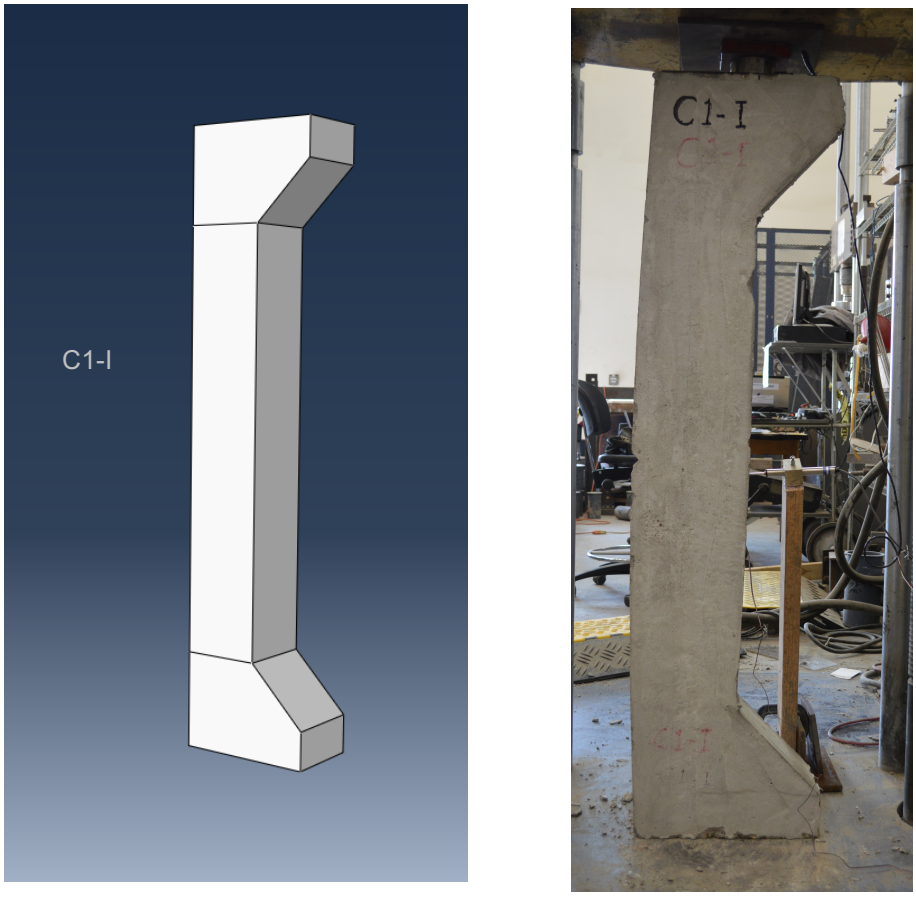

Figure 3.3 Concrete Column Modelled in Abaqus and Experimentally (Azzawi 2017)

3.3.2 Materials properties

Every part is made of a material. It is important to define the material, create section and assign the material properties associated to the respective part. When studying fracture, concrete is assumed to be a homogenous material.

3.3.2.1 Concrete

Density - 2400 kg/m3

Table 3.1 Change in concrete Physical Properties due to presence of Steel Fibers

Steel Fiber Content	Compressive Strength (f_c') [MPa]	Tensile Strength (f_t) [MPa]	Modulus of Elasticity (E) [MPa]
0%	30.90	3.31	26570
0.5%	32.75	3.60	27355
1.0%	34.53	4.14	28088
1.5%	35.25	4.50	28380

3.3.2.2 Steel Fibers

Table 3.2 Steel Fiber Physical Properties

Length[in]	Diameter [in]	Tensile Strength [ksi]
1.3	0.02	174

Figure 3.4 Steel Fibers used in the experiment (Azzawi 2017)

The above table and figure show the physical properties of the steel fibers used in the experiment (Azzawi 2017). In the numerical model, the fibers are not explicitly sketched and mixed with concrete. It is assumed that the effect of fibers is included by the increase in the tensile strength of the concrete. The tensile and compressive strength of concrete are obtained by the compressive strength test and split tensile strength test (Azzawi 2017).

In the numerical model, the fibers are not modelled explicitly. Their effect is assumed to be homogenous and is included in the column specimen by the change in concrete material properties. The most noticeable effect of adding steel fibers is the additional tensile strength it provides to the column specimen.

3.3.3 Load and Boundary conditions

The concrete column rests on a concrete pedestal. The pedestal has fixed boundary conditions. The interaction between the bottom surface of the column and the pedestal is of “Contact” Interaction.

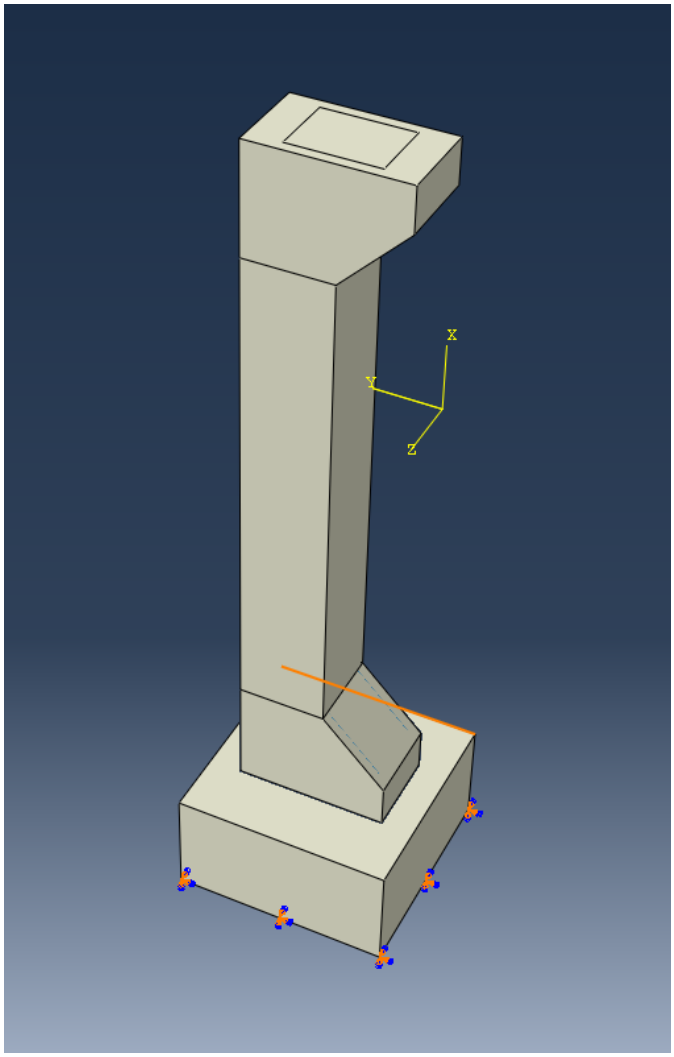

Figure 3.5 Concrete Column resting on pedestal having fixed boundary condition

The bottom surface of the column is the “Master” surface while the top surface of the pedestal is “Slave” Surface. Through this feature, a friction is developed between the two interfaces which is engaged on the application of load. Figure 3.4 shows a visual representation of the concrete column, pedestal and their boundary conditions.

Instead of applying load on the member. The top surface of the specimen is applied a distributed displacement in the direction of force. This is done to incorporate the non-linearity of the stress-strain curve. After attaining yield stress, the stress decreases while the strain increases in the stress-strain graph.

3.3.4 Steps

In the Abaqus software, the analysis comprises of various steps ranging from initial to the final step. It is up to the user to create and define the number of steps required. Each step can be customized as per the job requirements.

The initial step

Abaqus creates a special initial step at the beginning of the model's step sequence and names it 'Initial'. This default step is created by the software for the model, and it cannot be renamed, edited, replaced, copied, or deleted. The initial step allows the user to provide boundary conditions, predefined fields, and interactions that are applicable at the very beginning of the analysis.

Analysis Steps

The initial step is followed by one or more analysis steps. Each analysis step is associated with a specific procedure that defines the type of analysis to be performed during the step. After specifying the number of steps, it is essential to enter the total time period for the step.

3.3.5 Time Increment

Initial increment size: Abaqus starts the step using the value entered for the initial increment size. The value is 0.1.

Maximum increment size: The software will not increase the increment size beyond this value during the analysis. The value is 1.0.

Maximum number of increments: Abaqus limits the number of increments in a step to the value entered by the user for the maximum number of increments. If the step exceeds this number of increments, the analysis stops, and the diagnostic information is reported to the job module and written to the message file. By default, Abaqus sets the maximum number of increments to 100.

In Abaqus, every aspect of the result is measured with respect to time. So, load and displacement are initially displayed with respect to time. Both of this data is combined in the X-Y Data Manager of the Abaqus post-processor to obtain the Load-Displacement curve.

3.4 Plasticity Parameters for CDP Model

Concrete Damaged Plasticity

Among the inherent models available in Abaqus, Concrete Damage Plasticity CDP and Concrete Smeared Cracking models are capable of simulating concrete material properties. Concrete Smeared Cracking modelling of monotonic loading is suitable for situations where the confining pressure is less than four or five times the maximum uniaxial compression. In addition, Concrete Smeared Cracking has some problems with numerical convergence after the concrete cracking point is attained, specifically in cases where the whole system starts to unload after the initiation of the crack.

The Concrete damaged plasticity model is based on the assumption of scalar (isotropic) damage and is designed for applications in which the concrete is subjected to arbitrary loading conditions, including cyclic loading. The model takes into consideration the degradation of the elastic stiffness induced by plastic straining both in tension and compression. It also accounts for stiffness recovery effects under cyclic loading.

Concrete damage plasticity was first introduced by Lubliner et al to simulate the inelastic tensile and compressive behavior of concrete with the concept of isotropic damage elasticity and plasticity. A concrete damage plasticity model does not have the concept of crack at material integration points. This property of CDP model assumes that the cracking starts at points where the maximum principal strain is positive and the plastic strain is greater than zero.

The concrete damaged plasticity model considers the Poisson's ratio with a constant value for crack and un-cracked concrete. This value was considered as 0.2.

Wu et al. and Voyiadijis and Taqieddin recommend 31 to 42 degrees as the range of the dilation angle. Based on their recommendation, a dilation angle of 31 was chosen for this study. Kc is recommended to be more than 0.5, but less than or equal to 1 ($0.5 < Kf <= 1$). The default value should be 0.667.

Damage parameters were set to zero for both compression and tension behavior. They are more suitable for cases of brittle cracking behavior, whereas steel FRC presents a more ductile behavior than plain concrete. A zero-damage parameter leads to the consideration of both plastic and inelastic parameters as one. By this assumption, all the inelastic strains would be considered as cracking strain. In dynamic or cyclic loadings, it has been seen that the damage parameters are more important where the unloading needs to be defined by plastic strains. Ratio of biaxial to uniaxial compression (fb0/fc0) is recommended to be equal to 1.16.

Table 3.3 Concrete Damaged Plasticity Parameters values

Dilation Angle	**Eccentricity**	**fb0/fc0**	**K**	**Viscosity Parameter**
31	0.1	1.16	0.667	0

Chapter 4

Numerical Analysis

4.1 General

A preliminary study is done using ACI 318-14 guidelines to estimate the nominal load capacity and the ultimate load of the given sections. The nominal and ultimate capacities were determined for 0%, 10%, 20%, 25% and 30% hollow sections respectively. The voids were considered in the calculation by deducting the void area from the gross area of the cross-section. These calculations do not consider the effect of fibers. This procedure gives us an approximate strength value. The calculations are included in the Appendix A section of this thesis.

4.1 Mesh Convergence

A mesh convergence study was performed to select the optimum mesh (element) size. Different sizes of elements were selected and analyzed. Ultimately, the size, beyond which there was no considerable change in the results was selected as the desired element size.

A finer mesh requires a longer processing time for the Abaqus solver to run the analysis. While a larger mesh requires lesser processing time. However, a finer mesh provides more accurate results. So, the mesh convergence study takes into consideration all the above-mentioned factors and narrows the selection down to the optimum mesh size.

The basic steps towards converging to an optimum mesh size is as follows:

1. Create a mesh using the fewest, reasonable number of elements and analyze the model
2. Recreate the mesh with a denser element distribution, re-analyze it, and compare the results to those of the previous mesh.
3. Keep increasing the mesh density and re-analyzing the model until the results converge satisfactorily

At least three convergence runs will be required to plot a curve which can then be used to indicate when convergence is achieved or, how far away the most refined mesh is from full convergence. However, if two runs of different mesh density give the same result, convergence must already be achieved and no convergence curve is necessary.

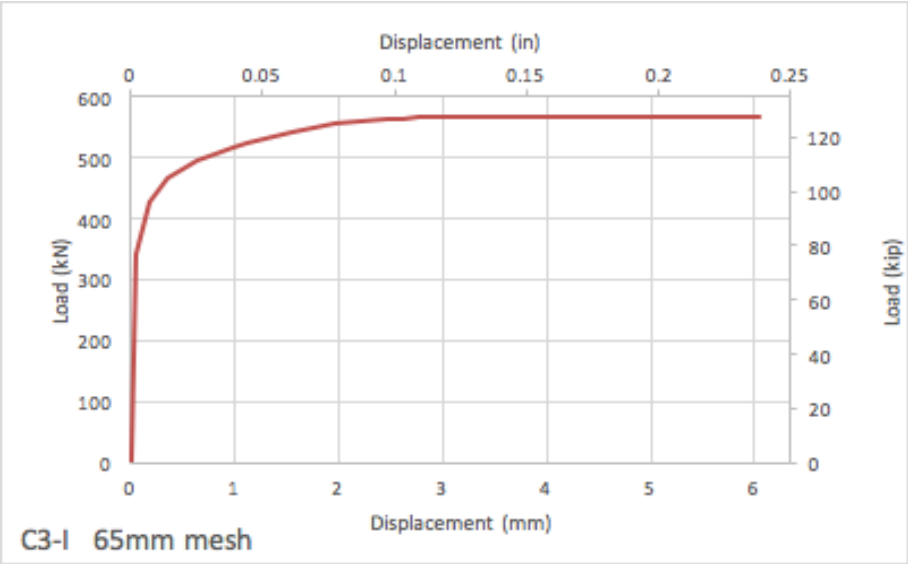

Figure 4.1 Load versus lateral mid-height deflection curve of specimen C3-I with a 65mm mesh size

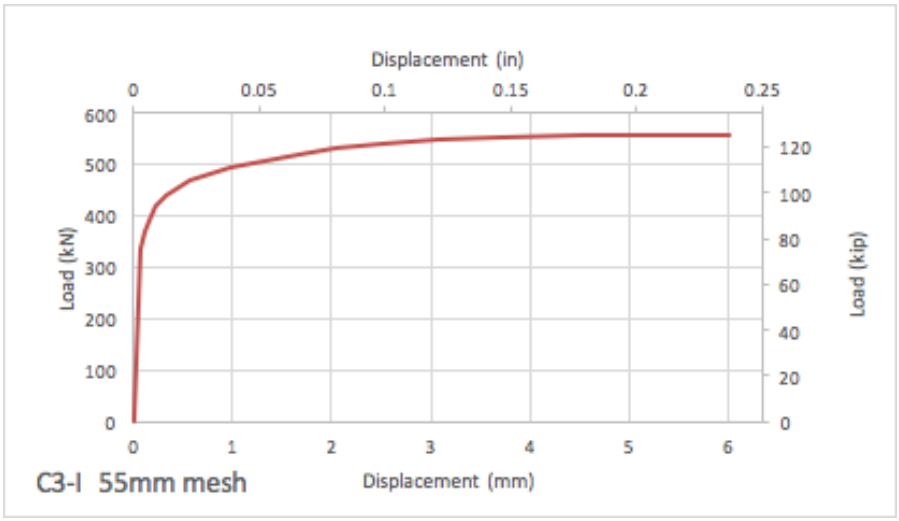

Figure 4.2 Load versus lateral mid-height deflection curve of specimen C3-I with a 55mm mesh size

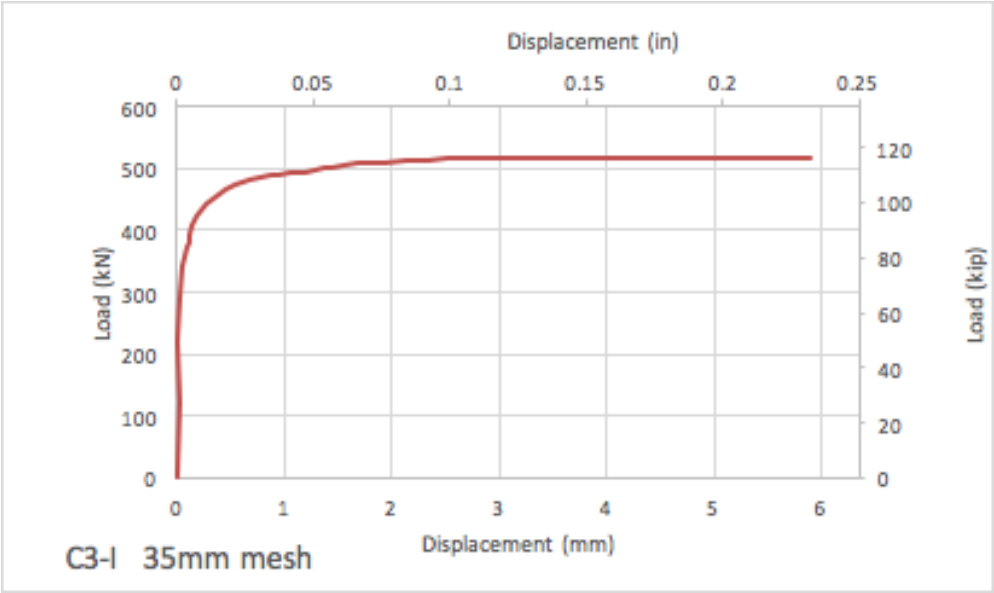

Figure 4.3 Load versus lateral mid-height deflection curve of specimen C3-I with a 35mm mesh size

By studying the results of three different mesh sizes, 35mm mesh size is selected as the optimum mesh size for analysis.

After selecting the optimum mesh size, we proceed to obtain the load - deflection curves for the specimens. The nomenclature of the specimens is as follows

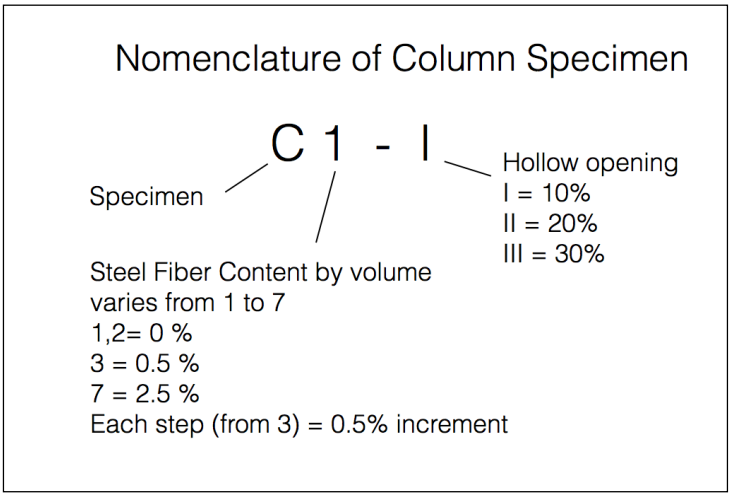

Figure 4.4 Nomenclature of Column Specimen

Table 4.1 Group I Specimen Description

Specimen	Cross-Section	Fiber Content
C1-I	Solid	0%
C2-I	10% Hollow	0%
C3-I	10% Hollow	0.5%
C4-I	10% Hollow	1.0%
C5-I	10% Hollow	1.5%

Table 4.2 Group II Specimen Description

Specimen	Cross-Section	Fiber Content
C1-II	Solid	0%
C2-II	20% Hollow	0%
C3-II	20% Hollow	0.5%
C4-II	20% Hollow	1.0%
C5-II	20% Hollow	1.5%

Furthermore, a parametric study was done in this study by varying two major parameters, the hollow opening percentage and steel fiber content percentage.

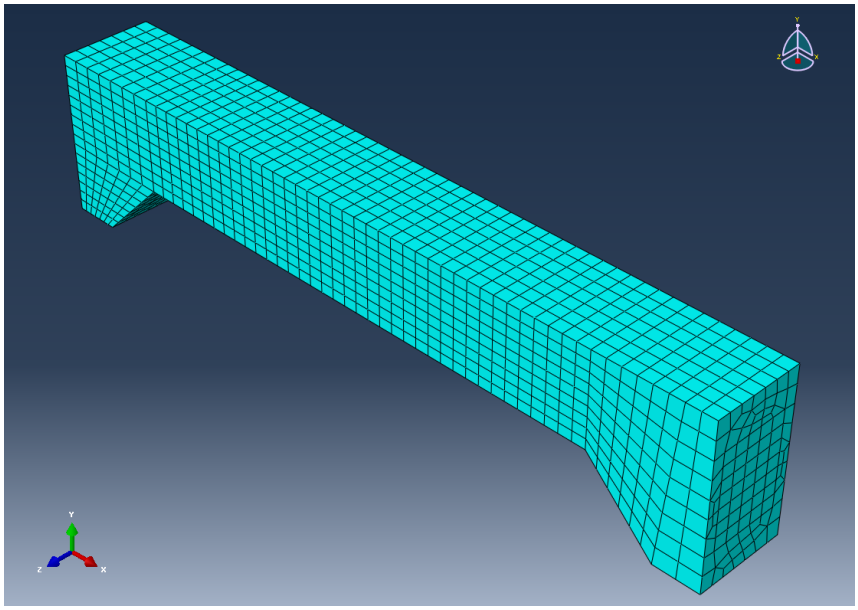

Figure 4.5 Meshed Specimen C1-I

An 8 noded linear hexahedral brick element with reduced integration and hourglass control was used to model the specimen in this study. There is no inherent set of units in Abaqus. It is up to the user to decide on a consistent set of units and use it throughout the modelling process.

4.2 Crack Propagation

After having decided the optimum mesh size, the job is created in Abaqus and it is submitted for analysis. Once the load application is initiated, the structure undergoes deformation up to the final collapse. The following are screen-captures from the post-processor of Abaqus.

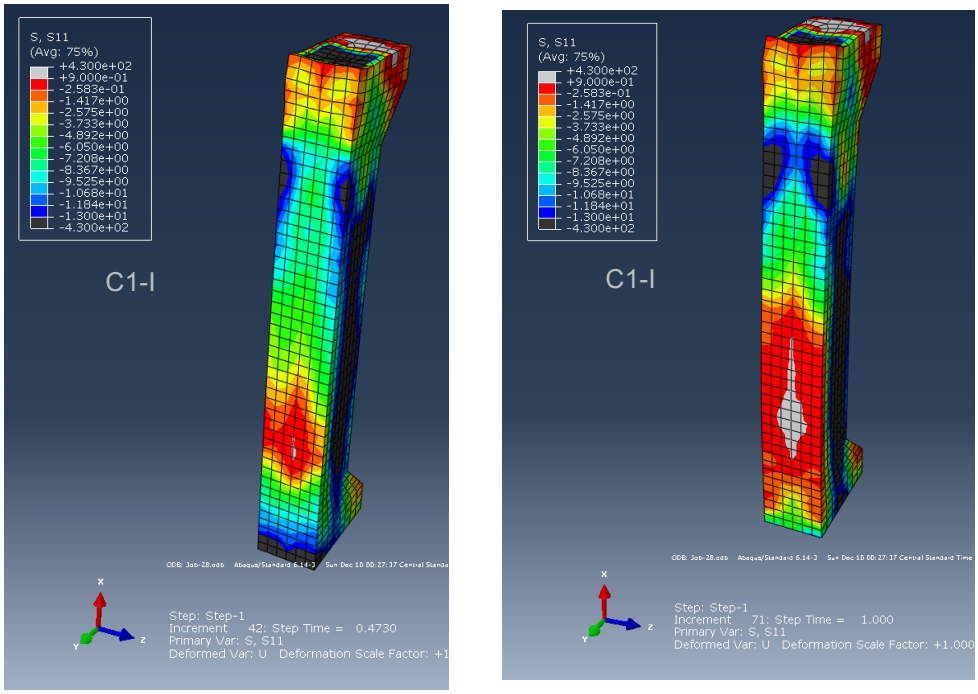

Figure 4.6 Crack propagation of specimen C1-I in Abaqus (top) and experiment (below)

The legend on the top left corner of Figure 4.6 shows the range of stresses in X direction. It is observed that the tensile cracks begin at time-interval step of 0.47. It is also important to observe the distribution of stresses at the column and bracket joint. The below Figure 4.7 shows a close up of section C3-I under applied maximum load. The blue/black region shows the region where compressive stresses are maximum and the red/grey region shows where tensile stresses are maximum.

The next figure shows a photograph of the specimen C1-I under applied load by the experiment conducted by Dr. Azzawi.

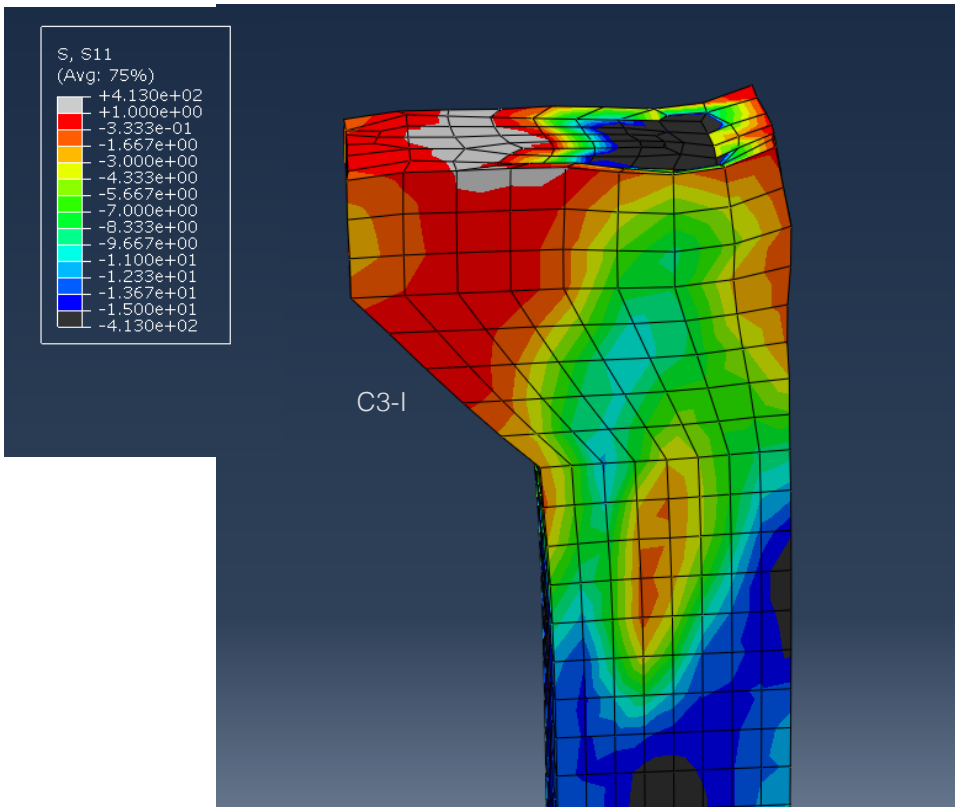

Figure 4.7 Specimen C3-I under applied load

Once the analysis is complete, Load - Deflection curves are plotted. The load is applied in the negative X direction and the Displacement is measured at the mid-height, mid-section of the column in the lateral Y direction. Abaqus provides X-Y Plot generator in the post-processor. The specific node at mid-height, mid-section is selected to determine the displacement and the Force in direction of load is selected. The two curves are combined to display one load versus lateral mid-height deflection curve, in which Force is on the Y axis and Displacement on X axis. Photographs of the concrete cylinders and few column specimens from the experiment are included in Appendix B section of this document.

4.3 Load Deflection Curves

In this section, the graphs obtained from Abaqus post-processor for Group I, Group II and the parametric study specimen are presented and discussed.

4.3.1 Group I Specimens

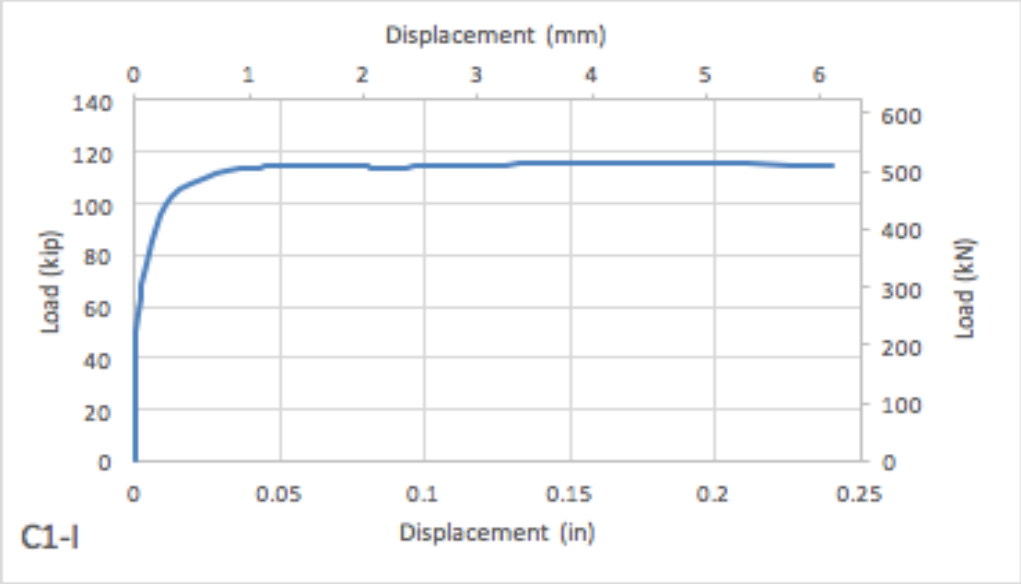

Figure 4.8 Load versus lateral mid-height deflection curve for specimen C1-I

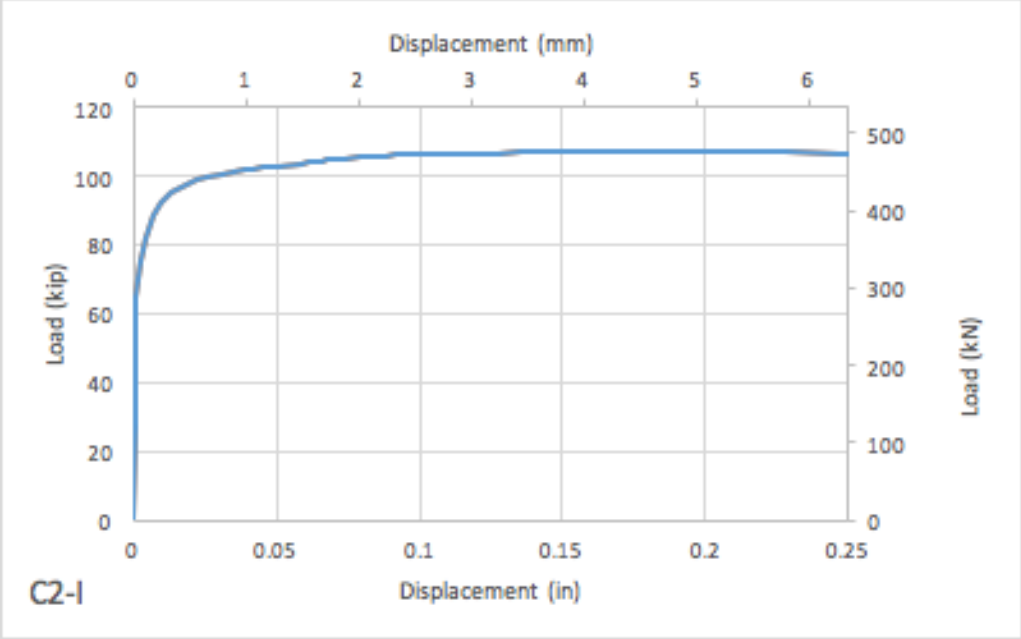

Figure 4.9 Load versus lateral mid-height deflection curve for specimen C2-I

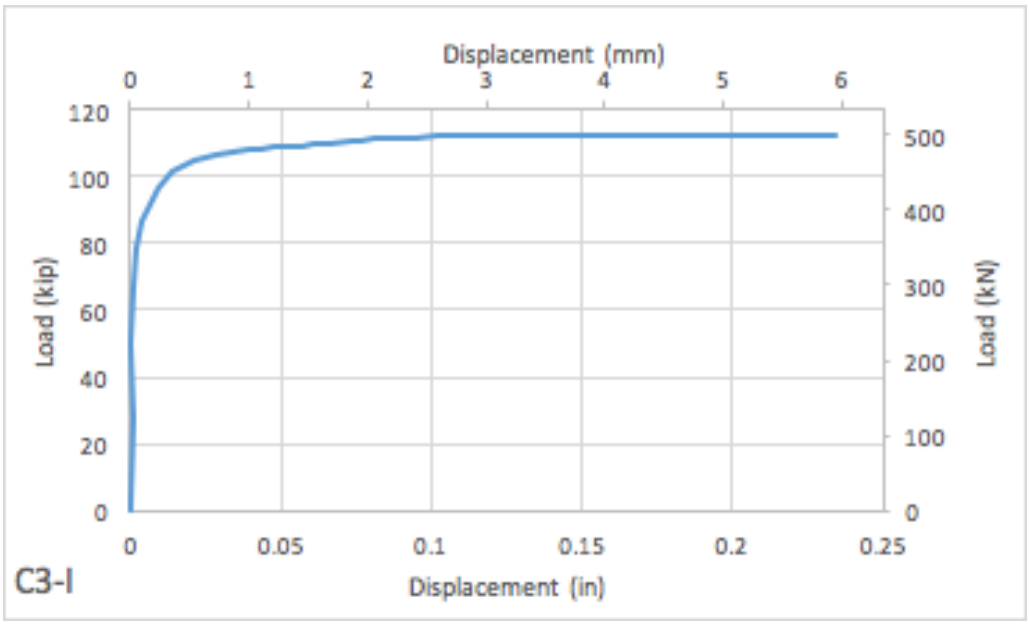

Figure 4.10 Load versus lateral mid-height deflection curve for specimen C3-I

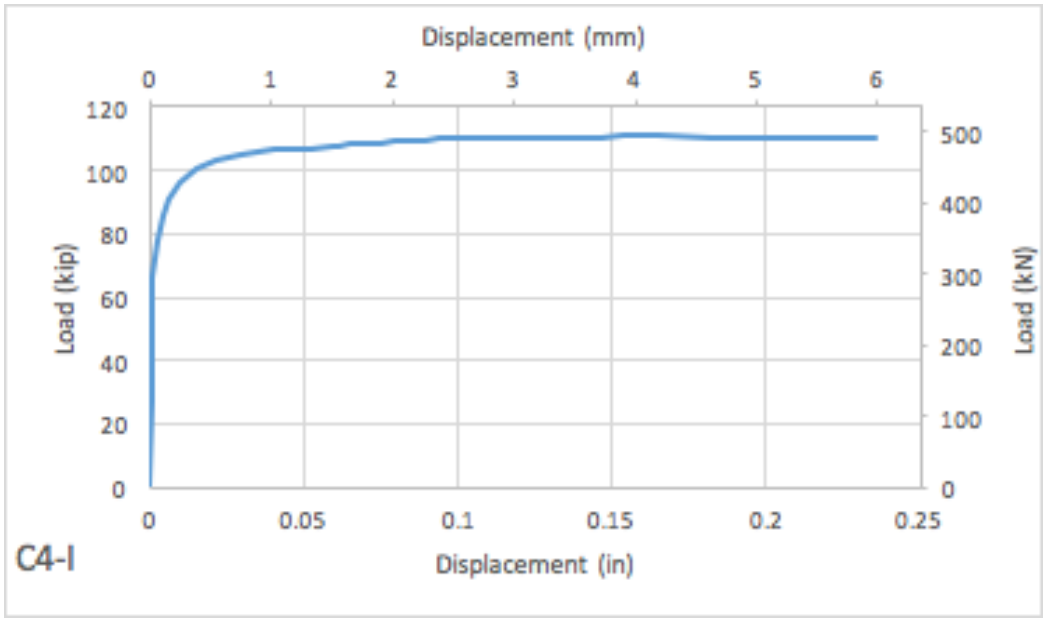

Figure 4.11 Load versus lateral mid-height deflection curve for specimen C4-I

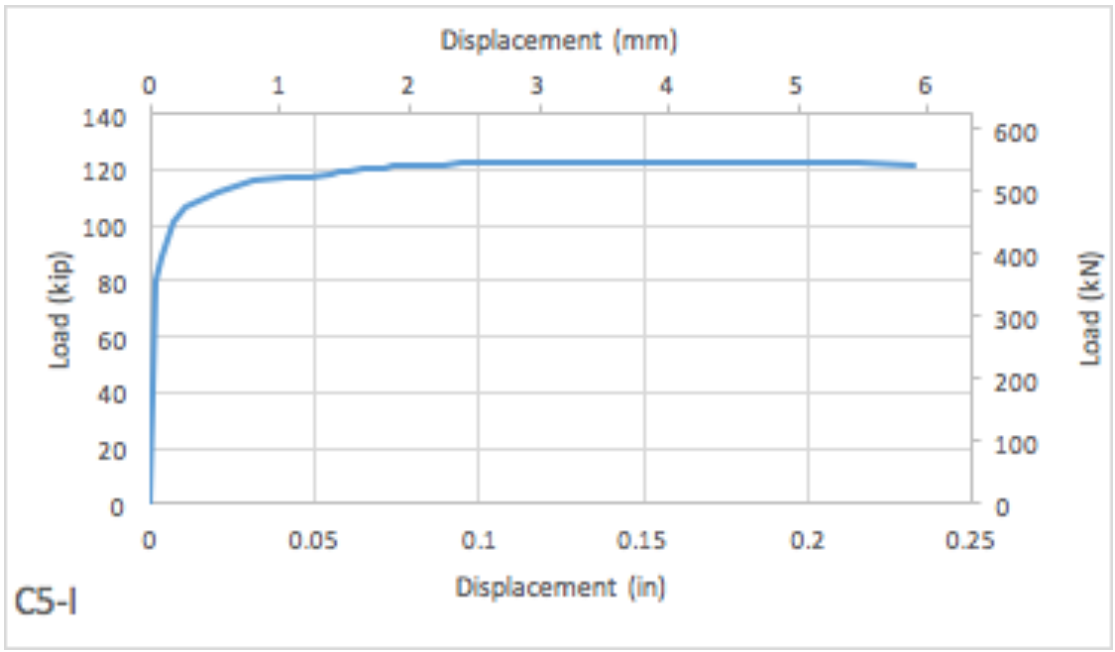

Figure 4.12 Load versus lateral mid-height deflection curve for specimen C5-I

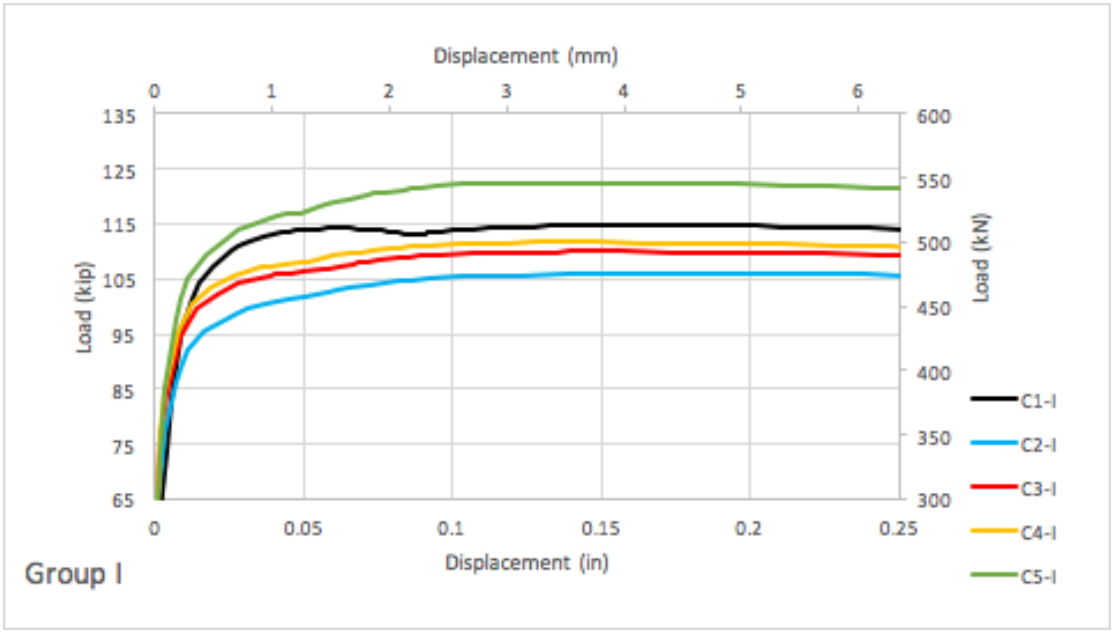

Figure 4.13 Load versus lateral mid-height deflection curve for Group I

Figure 4.13 shows a considerable drop in capacity by the introduction of hollow opening. This loss in strength is compensated by the addition of steel fibers.

Table 4.3 Group I Specimen Results

Specimen	Experimental Collapse Load (kip)	Numerical Collapse Load (kip)	Percentage Difference (%)	Average Percentage Difference (%)
C 1-I	110	117	6.36	6.164
C 2-I	105	111	5.81	
C3-I	109	115	5.5	
C 4-I	113	120	6.19	
C 5-I	115	123	6.96	

Table 4.3 shows the collapse load of all Group I specimen. The numerical results are compared to the Experimental collapse load values. The model is within 10% accuracy for the collapse load.

4.3.2 Group II Specimens

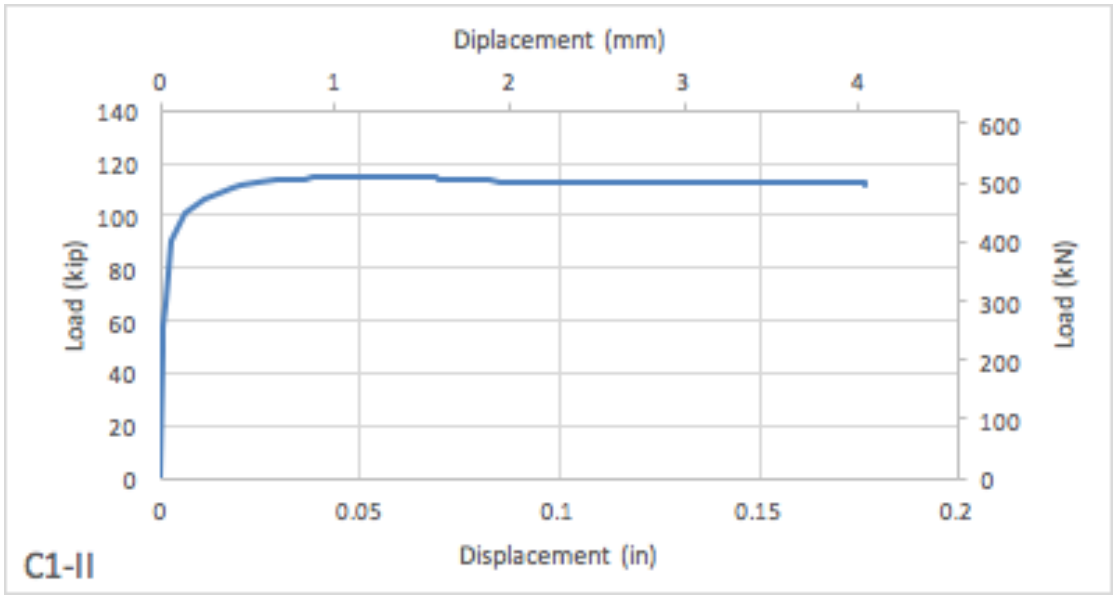

Figure 4.14 Load versus lateral mid-height deflection curve for Specimen C1-II

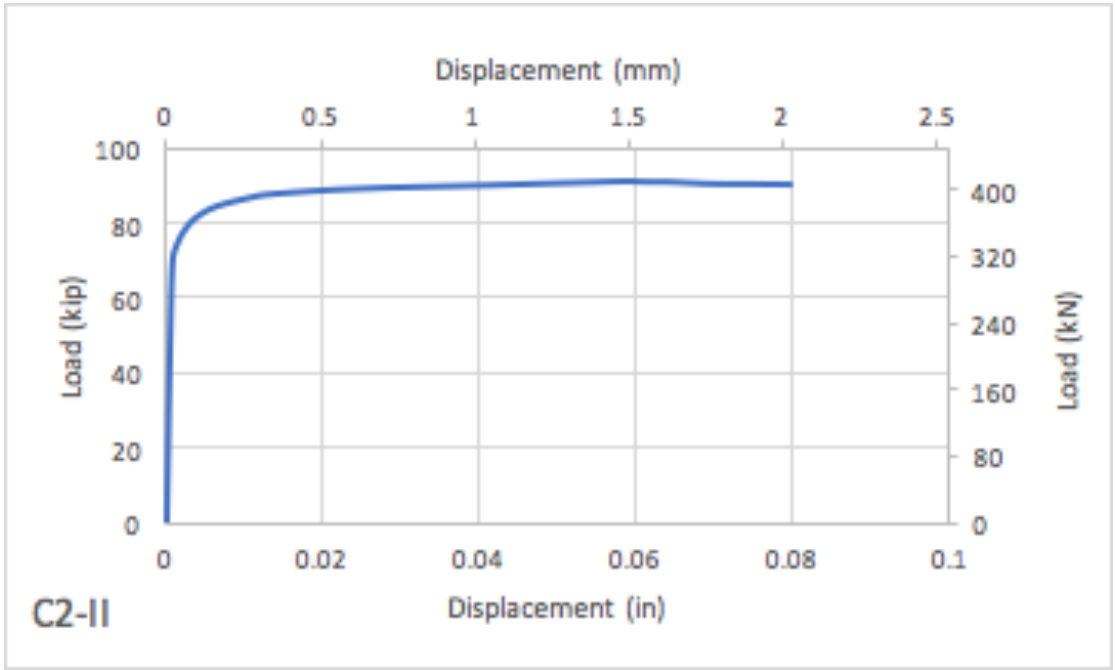

Figure 4.15 Load versus lateral mid-height deflection curve for specimen C2-II

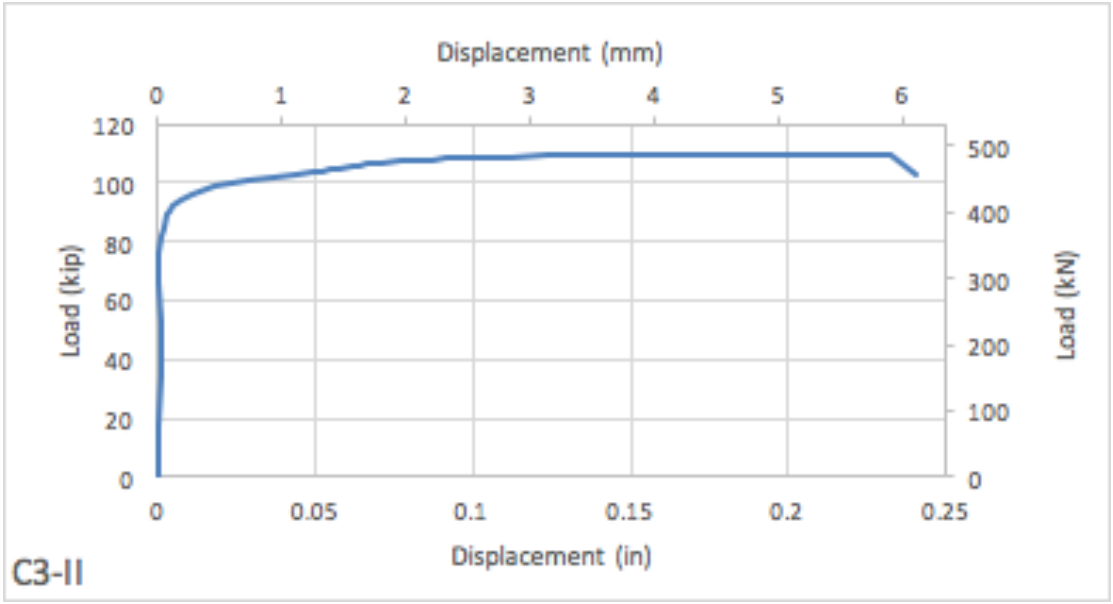

Figure 4.16 Load versus lateral mid-height deflection curve for specimen C3-II

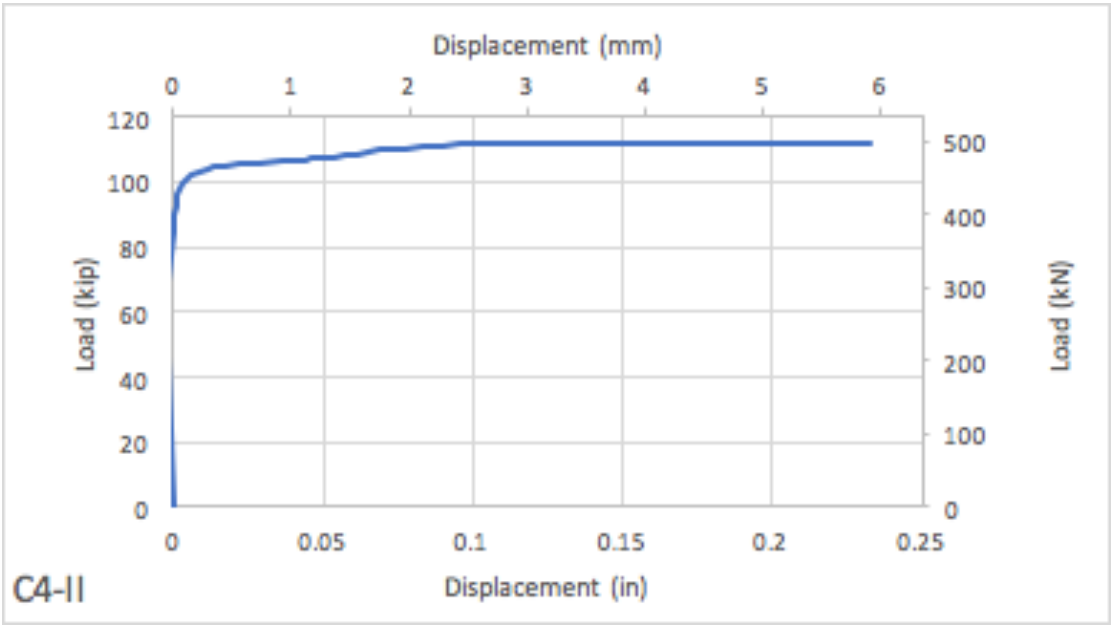

Figure 4.17 Load versus lateral mid-height deflection for specimen C4-II

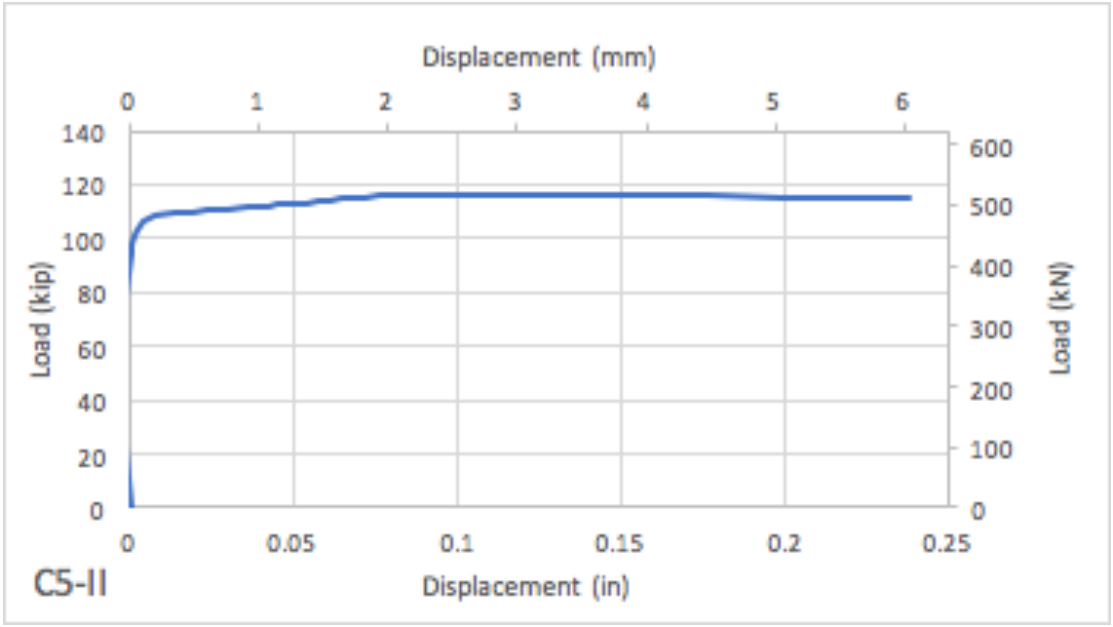

Figure 4.18 Load versus lateral mid-height deflection curve for specimen C5-II

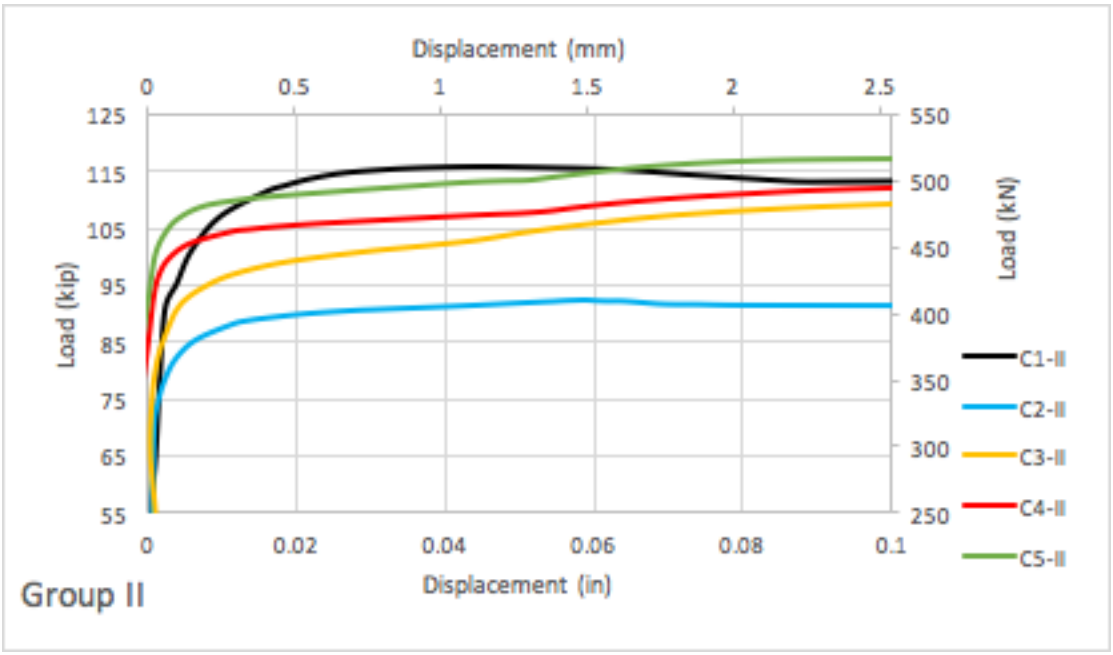

Figure 4.19 Load versus lateral mid-height deflection curve for Group II

On observation of Group II specimen graphs, a considerable difference is seen in C1-II and C2-II. This implies that introduction of a bigger void drops the capacity and also reduces the first-cracking load. However, the loss in strength is regained by addition of steel fibers and it is observed that the addition of 1.5% steel fibers by volume to a section having 20% void yields similar strength results to a solid section without any steel fibers.

Table 4.4 Group II Specimen results

Specimen	Experimental Collapse Load (kip)	Analytical Collapse Load (kip)	Percentage Difference (%)	Average Percentage Difference (%)
C 1-II	110	117	6.36	6.046
C 2-II	86	90	4.65	
C3-II	101	105	3.96	
C 4-II	103	109	5.83	
C 5-II	106	116	9.43	

Table 4.4 shows the collapse load of all Group II specimen. The numerical results are compared to the Experimental collapse load values. The model is within 10% accuracy for the collapse load.

4.3.3 Parametric Study

After the model was validated by comparing the analytical results to the experimental results, a parametric study was conducted by varying the hollow opening percentage and fiber content by volume percentage.

In the first parametric study, a 30% Hollow section was analyzed with steel fiber content of 0.5%, 1.0%, 1.5%, 2.0% and 2.5%. The load versus lateral mid-height deflection curves generated are as follows.

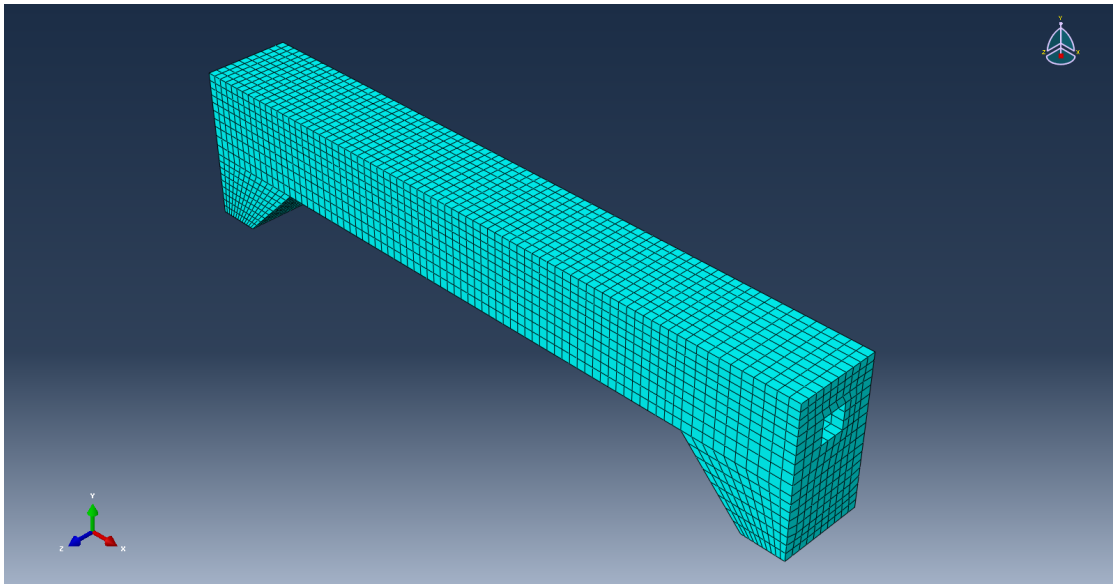

Figure 4.20 Meshed Parametric Specimen having 30% hollow section

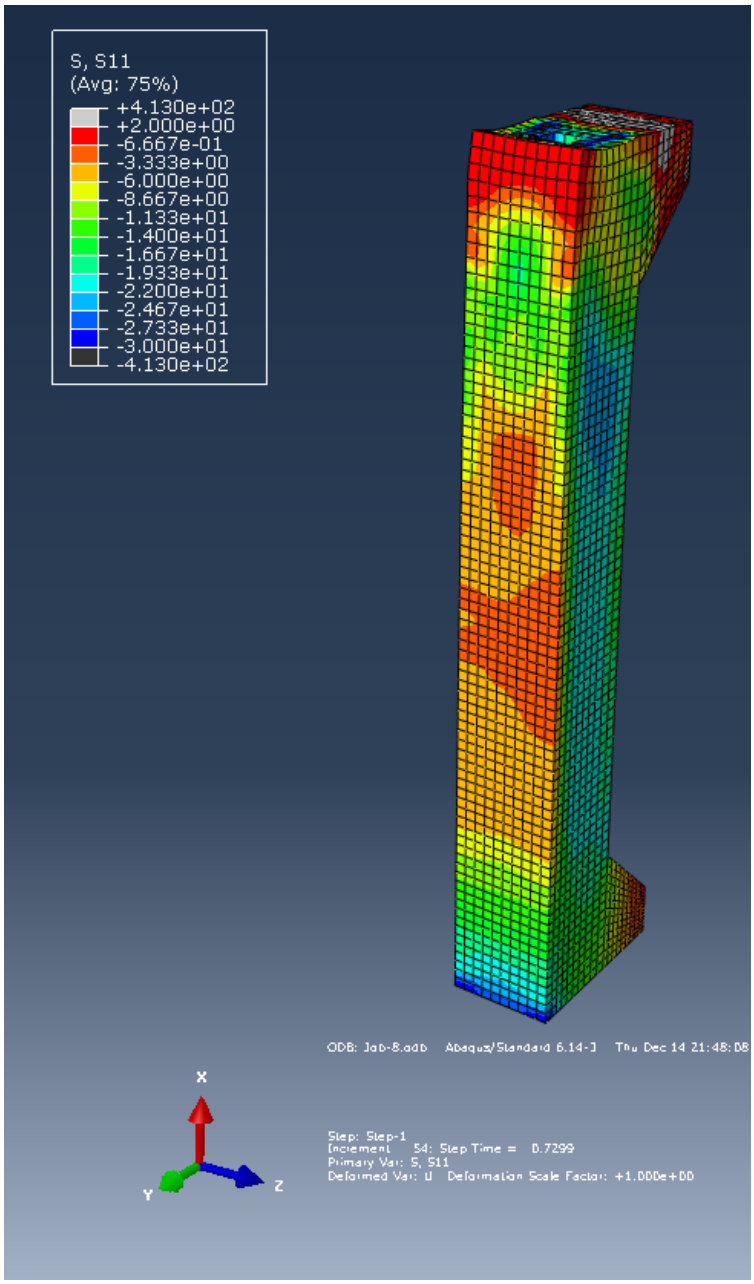

Figure 4.21 Stress distribution of Parametric Specimen under applied load

Figure 4.21 shows the distribution of stresses in the specimen having 30% hollow section. The blue/black regions show maximum compressive stress while red/grey regions show maximum tensile stresses.

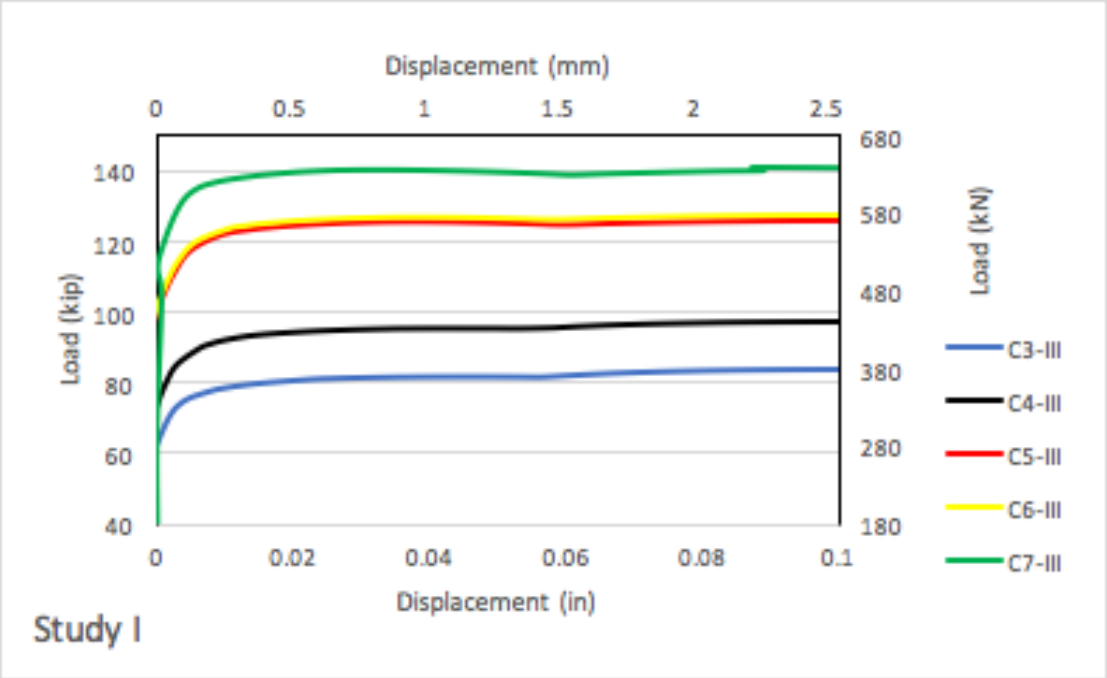

Figure 4.22 Load versus lateral mid-height deflection curve in Parametric Study I

Secondly, the steel fiber content was kept fixed at 1.5% and the hollow opening was varied from 10%, 20% and 30%, The load - displacement curve thus generated is as follows.

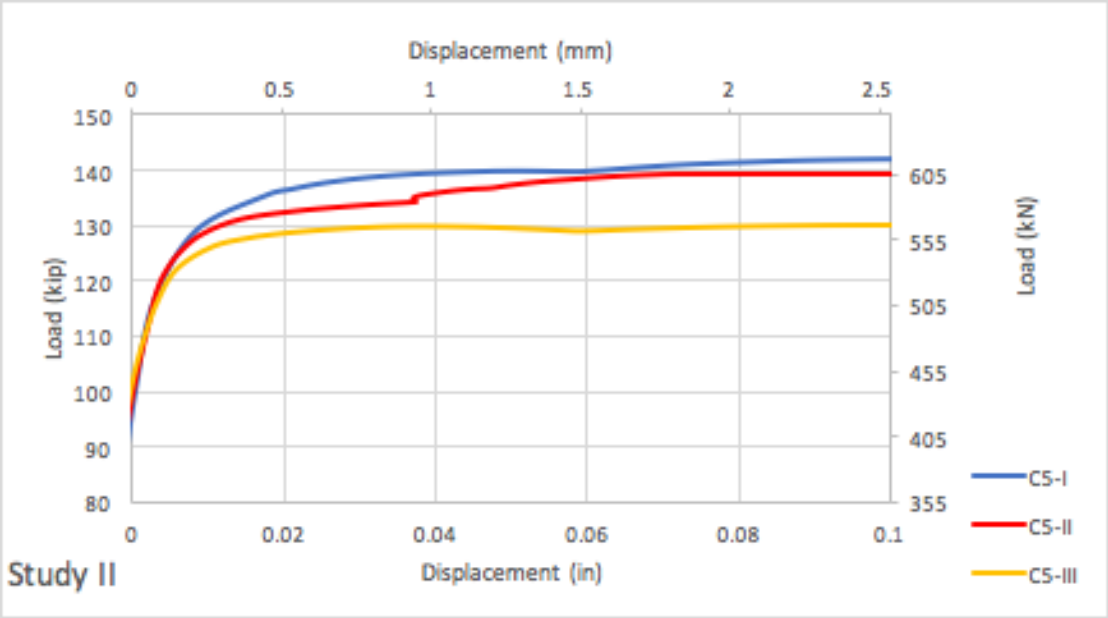

Figure 4.23 Load versus Lateral Mid-height Deflection Curve in Parametric Study II

Conducting the parametric study shows that increasing steel fiber content increases the first-cracking load and the ultimate capacity of the section. Also, increasing the hollow opening leads to sharp decline in the capacity of the section.

4.4 Discussion of Results

- The computer model was validated with the experiments to an accuracy of 6.15%.
- 10% Void in the section drops capacity by almost 5% and 20% Void in the section drops capacity by almost 20%.
- Generally, for small hollow openings (below 10% void), adding 0.5% steel fibers yields strength results close to a solid section without fibers.
- For openings within 20%, adding 1.5% steel fibers yields strength results close to a solid section without fibers.
- In all cases, it was observed that adding steel fibers increases the first-cracking load and the ultimate capacity of the section.

Chapter 5

5.1 Summary and Conclusions

This thesis documents a comprehensive investigation and analysis of eccentrically loaded hollow reinforced concrete columns with varying amounts of steels fibers. There were three types of sections in my study. Solid, 10% void and 20% void. Furthermore, a 30% hollow section was also studied.

- Adding steel fibers increases the hollow reinforced concrete columns first-cracking load and prevents premature failure of concrete cover and buckling outwards of steel bars.
- Adding steel fibers increases significantly the first-cracking load and allowing these columns to absorb energy greater than that needed to deform a similar column with ordinary reinforced concrete to the same load level.
- The strength and ductility improvements were more relevant in the case of specimens loaded with bigger steel fiber ratio added to concrete.
- For openings within 10%, adding 0.5% steel fibers by volume yields strength results similar to a solid section without any steel fibers.
- For openings within 20%, adding 1.5% steel fibers by volume yields strength results similar to a solid section without any steel fibers.
- From the parametric study, it was observed that for openings within 30%, adding 2.5% steel fibers by volume yields strength results similar to a solid section without any steel fibers.

5.2 Limitations of this Study

Several Limitations and assumptions were made for this study which are listed below

- The geometry of the column specimen was selected so as to keep it within the short column range.

- The column was subjected to axial compression and uniaxial bending by applying the compressive load at an eccentricity. However, torsional behavior of the section was not analyzed.
- The concrete used was normal weight and regular strength. The behavior may change when ultra-high strength concrete is used.

5.3 Recommendations for Future Work

- Use different material properties, for instance, high-strength concrete.
- Develop Load - Moment Interaction Diagrams.
- Select synthetic fibers, having different aspect ratios and study the results.
- Investigation of Performance of Slender Member.
- Vary load and boundary conditions.
- Investigate column to bracket joint behavior.
- Conduct sectional analysis for Hollow SFRC using ACI Code limitations and develop general formulae.

5.4 Summary

This study is aimed at investigating the performance of eccentrically loaded hollow columns with varying amounts of steel fibers. A total of 23 columns were analyzed using Finite Element Computer Application, Abaqus. Two parametric studies were conducted by varying the amount of void percentages and steel fiber contents. In the first study, a 30% hollow section was analyzed by varying steel fiber content in 0.5% increments from 0.5% to 2.5%. Secondly, the hollow opening for 10%, 20% and 30% was compared with a constant steel fiber of 1.5% by volume. The load versus lateral mid-height deflection curves were generated and results were close to the existing experimental data.

Appendix A

The following load calculations follow the ACI guidelines to obtain the Nominal load capacity and ultimate load capacity for 0%, 10%, 20%, 25% and 30% hollow sections. The area of the hollow section is deducted from the gross section of the concrete member.

Calculation for Nominal Load Capacity -- 0% Void

$A_g := 40000\ mm^2$
$A_s := 452.4\ mm^2$

$\frac{A_s}{A_g} = 0.011$ Minimum Longitudinal Steel Percentage is 1% of the Gross area of the section. Check

$A_n := A_g - A_s$
$A_n = (3.955 \cdot 10^4)\ mm^2$

$f_c' := 4\ ksi$ $f_c' = 27.579\ MPa$

$f_y := 30\ ksi$ $f_y = 206.843\ MPa$

Nominal Load Capacity

$P_o := 0.85 \cdot f_c' \cdot A_n + A_s \cdot f_y$
$P_o = 229.453\ kip$ $P_o = (1.021 \cdot 10^3)\ kN$

Ultimate Load

$\phi := 0.65$ Strength Reduction factor for Tied columns by ACI
$K := 0.8$

$P_u := \phi \cdot K \cdot P_o$
$P_u = 119.316\ kip$ $P_u = 530.742\ kN$

Calculation for Nominal Load Capacity -- 10% Void

$A_g := 39600\ mm^2$
$A_s := 452.4\ mm^2$

$\frac{A_s}{A_g} = 0.011$ Minimum Longitudinal Steel Percentage is 1% of the Gross area of the section. Check

$A_n := A_g - A_s$
$A_n = (3.915 \cdot 10^4)\ mm^2$

$f_c' := 4\ ksi$ $f_c' = 27.579\ MPa$

$f_y := 30\ ksi$ $f_y = 206.843\ MPa$

Nominal Load Capacity

$P_o := 0.85 \cdot f_c' \cdot A_n + A_s \cdot f_y$
$P_o = 227.345\ kip$ $P_o = (1.011 \cdot 10^3)\ kN$

Ultimate Load

$\phi := 0.65$ Strength Reduction factor for Tied columns by ACI
$K := 0.8$

$P_u := \phi \cdot K \cdot P_o$

$P_u = 118.219\ kip$ $P_u = 525.866\ kN$

Calculation for Nominal Load Capacity -- 20% Void

$A_g := 38400\ mm^2$
$A_s := 452.4\ mm^2$

$\frac{A_s}{A_g} = 0.012$ Minimum Longitudinal Steel Percentage is 1% of the Gross area of the section. Check

$A_n := A_g - A_s$
$A_n = (3.795 \cdot 10^4)\ mm^2$

$f_c' := 4\ ksi$ $f_c' = 27.579\ MPa$

$f_y := 30\ ksi$ $f_y = 206.843\ MPa$

Nominal Load Capacity

$P_o := 0.85 \cdot f_c' \cdot A_n + A_s \cdot f_y$
$P_o = 221.021\ kip$ $P_o = 983.15\ kN$

Ultimate Load

$\phi := 0.65$ Strength Reduction factor for Tied columns by ACI
$K := 0.8$

$P_u := \phi \cdot K \cdot P_o$
$P_u = 114.931\ kip$ $P_u = 511.238\ kN$

Calculation for Nominal Load Capacity -- 25% Void

$A_g := 37500\ mm^2$
$A_s := 452.4\ mm^2$

$\frac{A_s}{A_g} = 0.012$ Minimum Longitudinal Steel Percentage is 1% of the Gross area of the section. Check

$A_n := A_g - A_s$
$A_n = (3.705 \cdot 10^4)\ mm^2$

$f_c' := 4\ ksi$ $f_c' = 27.579\ MPa$

$f_y := 30\ ksi$ $f_y = 206.843\ MPa$

Nominal Load Capacity

$P_o := 0.85 \cdot f_c' \cdot A_n + A_s \cdot f_y$
$P_o = 216.278\ kip$ $P_o = 962.052\ kN$

Ultimate Load

$\phi := 0.65$ Strength Reduction factor for Tied columns by ACI
$K := 0.8$

$P_u := \phi \cdot K \cdot P_o$
$P_u = 112.464\ kip$ $P_u = 500.267\ kN$

Calculation for Nominal Load Capacity -- 30% Void

$A_g := 36400\ mm^2$
$A_s := 452.4\ mm^2$

$\frac{A_s}{A_g} = 0.012$ Minimum Longitudinal Steel Percentage is 1% of the Gross area of the section. Check

$A_n := A_g - A_s$
$A_n = (3.595 \cdot 10^4)\ mm^2$

$f_c' := 4\ ksi$ $f_c' = 27.579\ MPa$

$f_y := 30\ ksi$ $f_y = 206.843\ MPa$

Nominal Load Capacity

$P_o := 0.85 \cdot f_c' \cdot A_n + A_s \cdot f_y$
$P_o = 210.481\ kip$ $P_o = 936.266\ kN$

Ultimate Load

$\phi := 0.65$ Strength Reduction factor for Tied columns by ACI
$K := 0.8$

$P_u := \phi \cdot K \cdot P_o$
$P_u = 109.45\ kip$ $P_u = 486.858\ kN$

Appendix B

In this section, the experimental and photos are presented (Azzawi 2017).

Figure B1 Concrete Cylinder of specimens containing 0% steel fibers

Figure B2 Concrete Cylinder of specimens containing 0.5% steel fibers

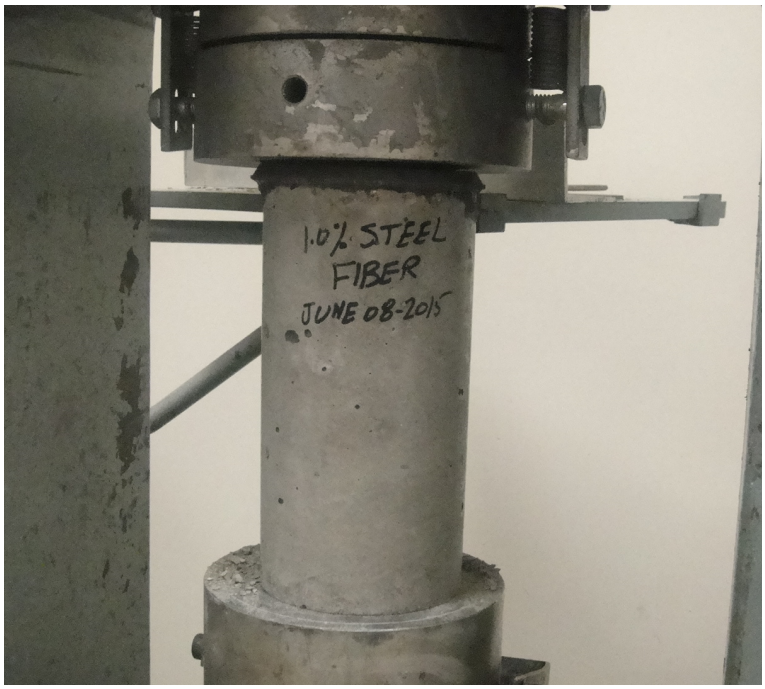

Figure B3 Concrete Cylinder of specimens containing 1.5% steel fibers

Figure B4 Concrete Cylinder of specimens containing 1.5% steel fibers

Figure B5 Concrete Cylinders for various specimens

Figure B6 Concrete Specimen being casted at the Laboratory

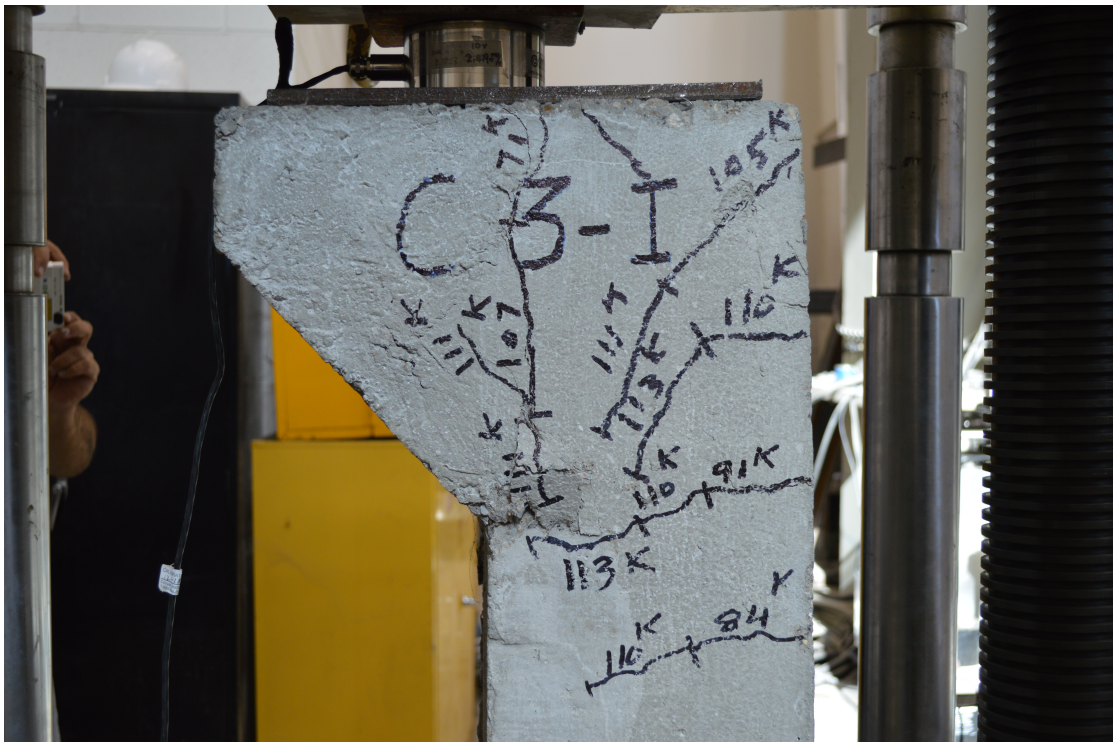

Figure B7 Specimen C3-I under applied load

Figure B8 Specimen C5-I under applied load

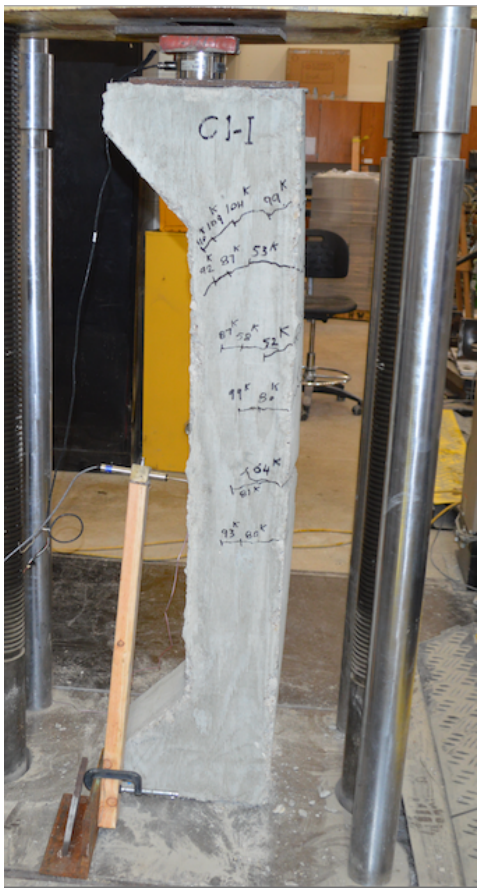

Figure B9 Specimen C1-I under applied load

Figure B10 Specimen C2-I under applied load

References

Raad Azzawi and Ali Abolmaali (2017) “Experimental Investigation of Steel Fiber Reinforced Concrete hollow column under eccentric loading.” Under Review.

AbdelAziz M. (2014) “Evaluation of the Performance of Steel Fiber Reinforced Concrete Pipes Produced by PackerHead Method.” University of Texas at Arlington.

Building and Code Requirements for Structural Concrete — ACI 318-14. ACI Committee.

S. A. Al-Ta’an, Mohammed and. Al-Jurmaa (2010) “Nonlinear Three Dimensional Finite Element Analysis of Steel Fiber Reinforced Concrete Deep Beam.” The Iraqi Journal For Mechanical And Material Engineering, Special Issue (E).

ABAQUS/CAE User’s Manual — ABAQUS Version 6.5 Documentation.

Daryl L. Logan (2007) “A First Course in the Finite Element Method.” Fourth Edition. University of Wisconsin—Platteville.

Tomasz J., Tomasz O. (2005) “Identification of Parameters of Concrete Damage Plasticity Constitutive Model.” Poznan University of Technology, Institute of Structural Engineering (ISE)

M. Nadim, Akthem A. (2015) “Structural Concrete Theory and Design” Sixth Edition. South Dakota State University, San Jose State University.

Siddharth A. Gaikwad (2017) “Analysis and Design of Hollow Reinforced Concrete Columns” Volume 5 Issue 4. International Journal on Recent and Innovation Trends in Computing and Communication.

Beck, Ryan, "Seismic behavior of hollow concrete columns" (2014). *Graduate Theses and Dissertations*. 14108.

David Tonseth and Kristian Welchermill “Design of Hollow Reinforced Concrete Columns in the Tubed Mega Frame” (2014). Master of Science Thesis KTH. Stockholm, Sweden.

Dr. Alaa K. Abdal Karim (2013). “Interaction of curves Proposed for Design and Analysis of Hollow Reinforced Concrete Columns”. Eng. & Tech Journal, Vol. 31.

Syed Faizuddin (2013). “Experimental Investigations on Strength Characteristics of High Strength Steel Fiber Reinforced Concrete with Mineral Admixtures” Structural Engineering, Department of Civil Engineering, DSCE, Bangalore.

Y. K Yeh (2002). “Seismic Performance of Rectangular Hollow Bridge Columns” ResearchGate.

Ho-Young Kim, Jae-Hoon Lee (2015). “Research for Hollow Reinforced Concrete Bridge Piers in Korea”. International Scholarly and Scientific Research & Innovation Vol. 9, No. 8.

Biographical Information

Huzaifa graduated from Visvesvaraya Tech. University in the spring of 2015, receiving a Bachelor of Engineering Degree in Civil Engineering. Soon after graduation he moved to Arlington Texas to pursue his Master Degree in Civil Engineering with a structural emphasis from the University of Texas at Arlington under the supervision of Dr. Raad Azzawi. Huzaifa plans to begin his career working for structural design firm in the North Texas region.